

Master in Chemical Engineering

***Test method development for textile helix cord
angle analysis***

Master's Thesis

by

Pedro Cordeiro Monteiro Pereira

Developed under the course of Dissertation

Performed at

Continental - Indústria Têxtil do Ave, S. A.



Supervisor from FEUP: **Prof. Adélio Mendes**

Supervisors from Continental-ITA: **Eng. Alexandre Gomes**

Dr. Thomas Kramer



Departamento de Engenharia Química

February 2016

Acknowledgements

Achieving a goal is nothing but the sum of all the steps taken towards it. It is now time to acknowledge those who allowed me to tread.

Firstly, to Mr. Eduardo Diniz and Mr. Manuel Pinheiro for the opportunity of developing my Master's Thesis in such a remarkable company as Continental-ITA.

To Eng. Alexandre Gomes and Dr. Thomas Kramer for the guidance and availability throughout the project.

To Professor Adélio Mendes for all the support, supervision and promising ideas regarding the test method development.

To Eng. Carla Pires, Eng. Diana Pinto and Eng. Ana Martins for the welcoming in the PI department and for always being available to answer any questions or doubts.

To my fellow interns, Raul Falcão, Mafalda Flores, Ângela Rodrigues, Ricardo Peixoto and Noman Mughal for the companionship throughout these months. Thank you for your helpfulness and for providing such a friendly and healthy working environment.

To my friends, for the support over these last years, and for making this journey so outstanding. A special thanks to Rita Matos, for the aid and helpfulness during this project.

To Nancy Curado, for the everyday motivation, optimism, cheer and support. Thank you for inspiring greatness.

Lastly, to my Parents and Family. Thank you for the unconditional support and for allowing me to pursue my dreams. I could not have a better role model than you, being this accomplishment not mine, but ours.

Abstract

This Master's Thesis was developed in the framework of a cooperation between Continental - Indústria Têxtil do Ave, S.A. (C-ITA) and the Faculty of Engineering of University of Porto (FEUP). Tires are highly engineered rubber-cord composites, with several components and layers. C-ITA is responsible for the manufacture of textile reinforcement materials used in tire construction.

Textile reinforcements display an essential role in tire performance. It is necessary a thorough study of textile cords characteristics and mechanical behavior. The objective of this project was the development of a test method for the visualization of textile cord elongation and the use of computer image analysis to measure the helix angles in the tested cords.

The first step taken towards the development of the test method was assembling and optimizing the test setup. For that, different video cameras and illumination sources were tested, as well as its placement and configuration. For the computer image analysis and the helix angle measurement, Tracker software was selected. Subsequently, the optimized setup and test procedure were determined.

Afterwards, the reliability of the measured helix angle values was assessed with the study of repeatability and operator influence. The helix angles of greige cords with different twist levels were measured and compared. It was concluded that as twist level increase the helix angle values also increase. The contributions of the material and structural deformations in cord elongation was studied through the analysis of helix angle evolution in load-elongation tests. Higher twist levels enhance the structural elongation in textile cords.

The influence of the dipping process in the helix angles was also studied. Due to the net stretch applied in the process, a reduction in the helix angle value was noticed. Besides the load-elongation tests performed, the helix angle behavior during mechanical hysteresis tests was studied.

The test method developed will not replace the standard load-elongation test, once it takes a considerable time to perform the image analysis. Although, it can provide tangible information concerning helix angles and the cord morphological behavior. It is a useful tool that allows further knowledge and understanding of the properties and behavior of the cords, and may aid in the study of less conventional cords such as unbalanced, asymmetrical and hybrid cords.

Key words: Tire, Textile reinforcements, Test method, Image analysis and Helix angle.

Resumo

Esta tese de mestrado foi desenvolvida através de uma cooperação entre a Continental - Indústria Têxtil do Ave, S.A. (C-ITA) e a Faculdade de Engenharia da Universidade do Porto (FEUP). Os pneus são materiais compósitos, compostos por vários componentes e camadas. A C-ITA é responsável pela produção de reforços têxteis usados na produção de pneus.

Os reforços têxteis cumprem uma função essencial no desempenho dos pneus. É necessário um estudo detalhado das características e propriedades mecânicas das cordas têxteis. O objetivo deste projeto foi o desenvolvimento de um método de teste para a visualização do alongamento das cordas têxteis e a medição dos ângulos das hélices através de análise de imagem.

A primeira fase no desenvolvimento do método de teste foi a montagem e otimização da instalação. Para tal, foram testadas várias câmaras de vídeo e fontes de iluminação, assim como a sua disposição. Para a análise de imagem e a medição dos ângulos das hélices foi usado o *software* Tracker. Desta forma, o procedimento do método de teste foi determinado.

Posteriormente, foram determinadas a repetibilidade e influência do operador nos valores dos ângulos das hélices medidos. Cordas verdes com diferentes torções foram testadas. Comparando os valores dos ângulos das hélices, registou-se que com o aumento da torção das cordas, o valor do ângulo das hélices também aumenta. Através da análise da evolução dos ângulos das hélices ao longo de testes força-alongamento, foi estudada a contribuição da deformação estrutural e material na corda. Torções maiores aumentam a contribuição da deformação estrutural nas cordas têxteis.

A influência do processo de impregnação nos ângulos das hélices foi também alvo de estudo. Devido ao estiramento aplicado à corda no processo, foi registada uma redução no valor dos ângulos das hélices. Além dos testes força-alongamento, também foi estudada a evolução dos ângulos das hélices durante um teste de histerese mecânica.

O método de teste desenvolvido não substituirá o teste força-alongamento ordinário, uma vez que a análise de imagem demora um tempo considerável para ser efetuada. Contudo, pode fornecer informação importante relativamente ao comportamento morfológico das cordas têxteis. É assim uma ferramenta útil, que permite desenvolver conhecimento e compreender melhor o comportamento das cordas. Pode também desempenhar um papel importante no estudo de cordas menos convencionais, como cordas híbridas, assimétricas e não balanceadas.

Palavras-chave: Pneu, Reforços têxteis, Método de teste, Análise de imagem e Ângulo da Hélice.

Statement

I hereby declare, on oath, that this work is original and that all non-original contributions were properly referenced with identification of the source.

1st February 2016

(Pedro Cordeiro Monteiro Pereira)

Index

1	Introduction.....	1
1.1	Project presentation and framework	1
1.2	Work contributions	5
1.3	Thesis organization	5
2	State of the Art.....	6
2.1	Reinforcement materials	6
2.2	Textile reinforcement manufacture	8
2.2.1	Twisting.....	9
2.2.2	Weaving.....	11
2.2.3	Dipping	11
2.3	Video analysis.....	13
3	Materials and Methods	15
3.1	Equipment.....	15
3.1.1	Video recording equipment	15
3.1.2	Laboratory twisting unit	16
3.1.3	Twist tester	16
3.1.4	Laboratory dipping unit	17
3.1.5	Tensile machine	18
3.2	Technical procedure and conditions	18
4	Results and Discussion	20
4.1	Installation setup.....	20
4.2	Image analysis setup.....	23
4.3	Test method application.....	26
5	Conclusions	39
6	Project Assessment.....	40
6.1	Limitations and future work	40

6.2 Final assessment 40

7 References 41

8 Attachment I - Test Method Procedure 43

List of Figures

Figure 1 - Materials used in a tire (adapted from [2]).	1
Figure 2 - Tire forces and moments acting at the center of tire contact (adapted from [7]).	2
Figure 3 - Tire structural composition (adapted from [2]).	3
Figure 4 - Hybrid cord constitution (adapted from [19]).	8
Figure 5 - Stress-strain curves of tire reinforcement materials (adapted from [20]).	8
Figure 6- Twist directions (adapted from [19]).	9
Figure 7 - Principles of twisting: a) twisting process (adapted from [19]) and b) twisting system (adapted from [20]).	10
Figure 8 - Helix angle exemplification (adapted from [1]).	10
Figure 9 - Basic loom arrangement (adapted from [20]).	11
Figure 10 - Dipping and Heat treatment process (adapted from [20]).	12
Figure 11 - Textile cords with different twist levels (a) 200 tpm, (b) 400 tpm, and (c) 550 tpm.	13
Figure 12 - Digital camera mechanism (adapted from [28]).	13
Figure 13 - Different cameras used in the development of the test method: a) Logitech, b) EdmundOptics and c) Pentax WG-III.	15
Figure 14 - Artificial light sources used: a) led flashlight and b) led spotlight.	15
Figure 15 - Laboratory Twisting Unit.	16
Figure 16 - Zweigle twist tester.	17
Figure 17 - Laboratory Dipping Unit.	17
Figure 18 - Zwick Roell tensile test machine.	18
Figure 19 - Load-elongation test (adapted from [19]).	19
Figure 20 - Images obtained with different cameras: a) EdmundOptics, b) Pentax WG-III and c) Logitech.	20
Figure 21 - Influence of proper illumination enhancement: a) without controlled illumination and b) with controlled illumination.	21
Figure 22 - Tracker software user interface.	22
Figure 23 - Installation setup of the test method.	22
Figure 24 - Measured helix angle (θ) disambiguation.	23
Figure 25 - Zwick elevation device.	24
Figure 26 - Zwick elevation device: a) test beginning and b) test end.	25

<i>Figure 27 - Helix angle vs Twist level at pre-tension.</i>	<i>28</i>
<i>Figure 28 - Helix angle vs Twist level at LASE 2 %.</i>	<i>28</i>
<i>Figure 29 - Helix angle vs Twist level at LASE 4 %.</i>	<i>29</i>
<i>Figure 30 - Helix angle vs Twist level at the moment of break.</i>	<i>29</i>
<i>Figure 31 - Load-elongation curves of cords with different twist level.</i>	<i>30</i>
<i>Figure 32 - Helix angle profile for greige 200 tpm cord.</i>	<i>31</i>
<i>Figure 33 - Helix angle profile for greige 400 tpm cord.</i>	<i>31</i>
<i>Figure 34 - Helix angle profile for greige 550 tpm cord.</i>	<i>31</i>
<i>Figure 35 - Load-elongation curves of greige cords with different twist levels.</i>	<i>32</i>
<i>Figure 36 - Load-elongation curve of dipped and greige cords with different twist level.</i>	<i>33</i>
<i>Figure 37 - Helix angle profile for greige and dipped 200 tpm cord.</i>	<i>34</i>
<i>Figure 38 - Helix angle profile for greige and dipped 400 tpm cord.</i>	<i>34</i>
<i>Figure 39 - Helix angle profile for greige and dipped 550 tpm cord.</i>	<i>35</i>
<i>Figure 40 - Normalized helix angle profile at different times.</i>	<i>36</i>
<i>Figure 41 - Nylon mechanical hysteresis.</i>	<i>36</i>
<i>Figure 42 - Helix angle at 2 % elongation.</i>	<i>37</i>
<i>Figure 43 - Helix angle at 4 % elongation.</i>	<i>37</i>
<i>Figure 44 - Frame-by-frame cord breaking mechanism.</i>	<i>38</i>
<i>Figure 45 - Frame-by-frame cord breaking mechanism on hybrid cord.</i>	<i>38</i>
<i>Figure 46 - Video synchronization by laser light detection.</i>	<i>44</i>
<i>Figure 47 - testXpert user interface for video analysis.</i>	<i>44</i>
<i>Figure 48 - Tracker user interface.</i>	<i>45</i>
<i>Figure 49 - Protractor displacement exemplification.</i>	<i>46</i>
<i>Figure 50 - Helix angle measurement exemplification.</i>	<i>46</i>

List of Tables

<i>Table 1 - Dipping conditions used in LDU.</i>	<i>19</i>
<i>Table 2 - Repeatability of the image analysis.</i>	<i>25</i>
<i>Table 3 - Operator influence on helix angle measurement in greige cords.</i>	<i>26</i>
<i>Table 4 - Operator influence on helix angle measurement in dipped cords.....</i>	<i>26</i>
<i>Table 5 - Twist level influence in the helix angle in greige cords.</i>	<i>27</i>
<i>Table 6 - Twist level influence in the helix angle in dipped cords.....</i>	<i>33</i>

Glossary and Acronyms

σ	load	N
σ_0	pre-tension	N
ε	elongation	%
$\varepsilon_{at\ break}$	elongation at break	%
$dtex$	decitex	g/10,000 m
α	helix angle	°
α_0	helix angle at pre-tension	°
$\alpha_{at\ break}$	helix angle at break	°

List of Acronyms

C-ITA	Continental - Indústria Têxtil do Ave, S.A.
FEUP	Faculty of Engineering of University of Porto
LTU	Laboratory Twisting Unit
LDU	Laboratory Dipping Unit
CCD	Charge-Coupled Device
LASE	Load At Specific Elongation
ASTM	American Society for Testing and Materials
PET	Polyethylene terephthalate

1 Introduction

1.1 Project presentation and framework

The wheel is considered one of the most important inventions throughout the human history [1]. For more than 5 000 years it has been reinvented at different times and locations to meet current transportation needs [2].

The rudimentary concept of tire consisted in a leather layer to prevent damage to the wooden wheel frame. The pneumatic tire was invented in 1888 by John Dunlop, initially for bicycles and afterwards for automobiles. The industrialization in Europe and North America, and the discovery of vulcanization by Charles Goodyear, enabled the tire to evolve from a rubberized canvas covering a rubber tube to a complex fabric, steel, and elastomeric composite [1-3].

Tires are highly engineered structural composites made of up to 20 components parts and as many as 15 different rubber compounds [4]. The materials used in the tire construction are presented in Figure 1.



Figure 1 - Materials used in a tire (adapted from [2]).

Tires are undoubtedly the most critical safety component on a vehicle. They affect traction, handling, steering, braking, cushion and stability. Even in adverse conditions, tires must be capable of transmitting strong longitudinal and lateral forces, assuring optimal and reliable roadholding quality [2, 5]. As tires are the interface between vehicle and road, they support all the vehicle load, are responsible for surface friction and for absorbing road irregularities [4, 6]. Therefore, tires are highly engineered structural composites with an enormous endurance requirement. Every tire component experiences more than 40 million loading-unloading cycles [4]. The mechanical properties of a tire describe its response to the application of load, torque,

and steering input, resulting in the generation of external forces and deflection [1]. The result is a complex set of forces acting on a rolling tire, represented in Figure 2.

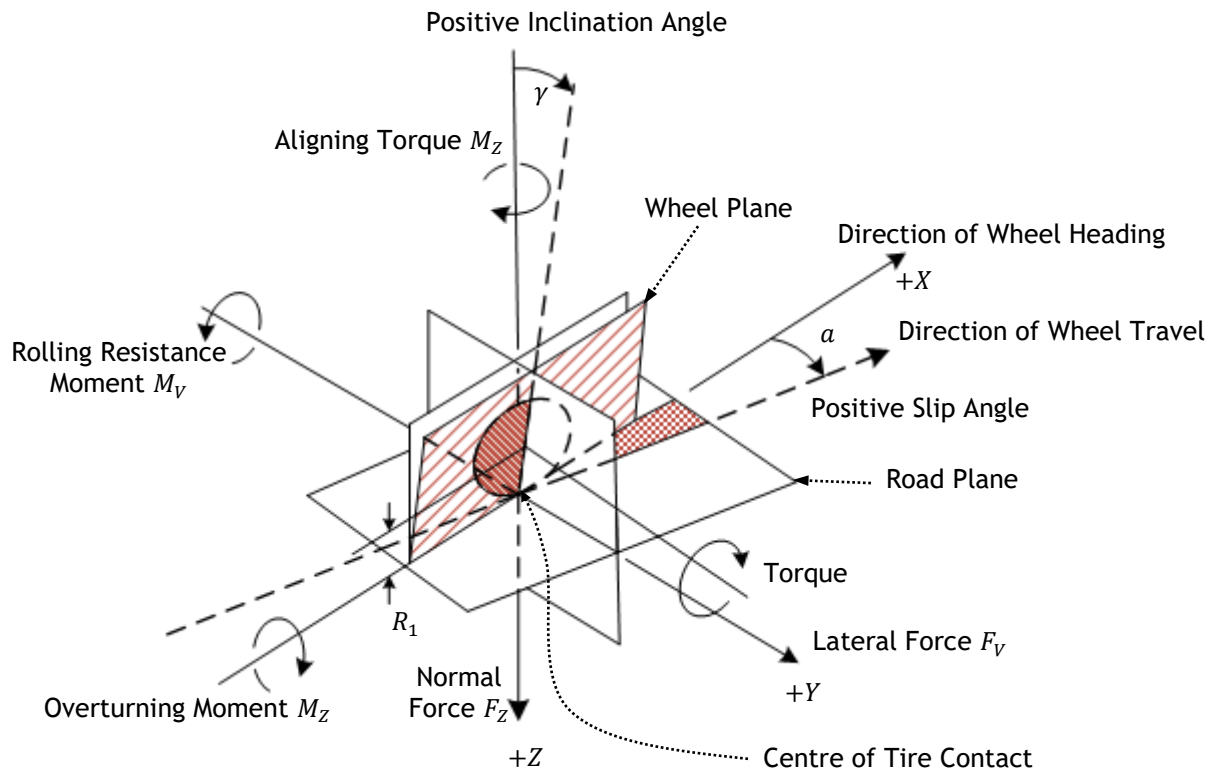


Figure 2 - Tire forces and moments acting at the center of tire contact (adapted from [7]).

A tire is essentially a cord-rubber composite, being the displacement of the reinforcement materials a crucial matter, as they are responsible for the major part of the tire's mechanical properties. Nowadays, the tire most commonly produced is the radial (or belted) tire [2]. This arrangement has the advantage of granting an easier deflection under load, thus reducing the generation of heat, reducing the rolling resistance and improving high-speed performance. On the other hand, due to its complex construction, it increases material and manufacturing costs [4].

The structure of a modern radial car tire is represented in Figure 3.

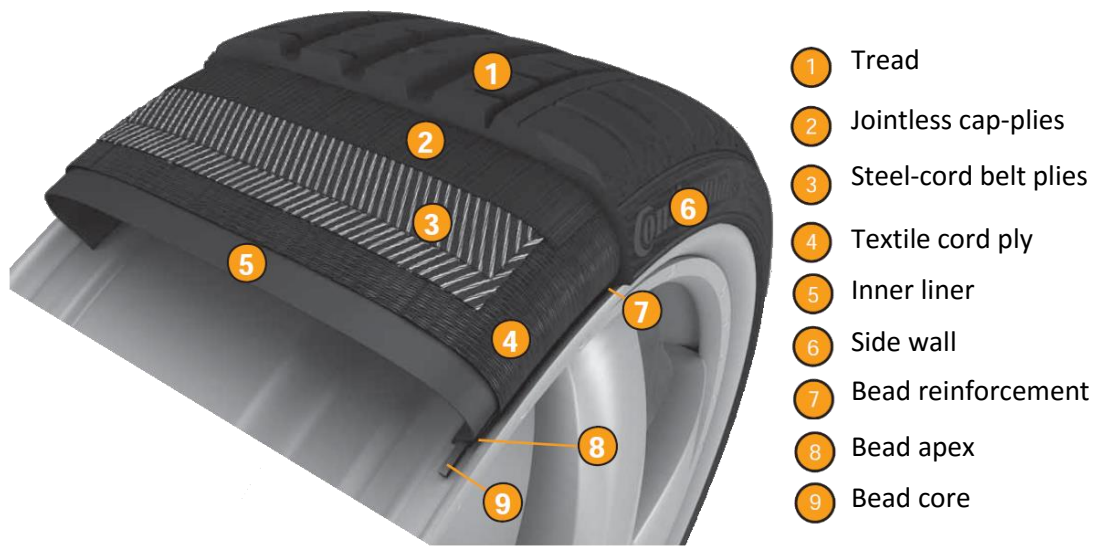


Figure 3 - Tire structural composition (adapted from [2]).

The tread is made from a hard wearing rubber compound in order to be tough, resilient and minimize damage to the casing. It is also responsible for providing grip on all road surfaces and directional stability. A pattern is molded into the tread during vulcanization, and it is designed to provide uniform wear, to channel water out of the footprint, and to minimize pattern noise [2, 4, 8].

Jointless cap-ply provides an additional contractive force to resist any growth of the belt edges due to centrifugal forces and temperature increase. Normally are constituted of nylon embedded in rubber [2, 9].

Two steel cord-belt plies are applied at opposite angles to one another between the jointless cap-ply and the textile cord ply. It enhances shape retention, directional stability, and provides impact resistance. The angle formed by the two layers affects vehicle ride and handling characteristics [2, 4].

Textile cord ply is disposed radially across the tire and is responsible for keeping internal pressure and the tire's shape. Underneath it, the inner liner improves air retention by lowering permeation outwards through the tire [2, 4, 9].

Tire sidewall serves to protect the body plies from external damage and atmospheric conditions [2, 4]. The bead apex and the bead reinforcements (or sidewall reinforcements) provide steering precision and enhance directional stability [2, 4, 8, 9]. Finally, the bead core is made of steel wire and ensures that the tire sits firmly on the rim and prevent air leakages [2].

Continental AG was founded in 1871 in Hannover, Germany. It started producing soft rubber products, rubberized fabrics, and solid tires for carriages and bicycles. The production of pneumatic tires started in 1898. Nowadays the Continental Corporation is divided into the Automotive Group and the Rubber Group, and consists of five different divisions: Chassis & Safety, Powertrain, Interior, ContiTech and Tires [10]. With the purpose of developing intelligent technologies for transporting people and their goods, Continental aims to improve mobility making it sustainable, safer, comfortable and affordable. In 2014, Continental ranked among the top 3 automotive suppliers worldwide [11]. Currently the company employs over 130 000 people in 38 countries, generating sales of approximately 34 500 million euros [12].

Continental - Indústria Têxtil do Ave, S.A. (C-ITA) was founded in 1950 in Lousado, Portugal. Began operating as a cluster company with Mabor and became part of Continental AG in 1993 [10]. C-ITA is responsible for the transformation of greige yarn into high-value dipped cord and fabric, required to grant to the tire important mechanical properties. Reinforcement materials are responsible for carrying the major part of the structural load of the automobiles and should exhibit excellent dimensional stability, tensile and fatigue properties [1, 4, 13, 14]. Alongside C-ITA, there is only one more facility (located in the United States of America) producing textile reinforcements used in Continental tires.

In tire development, knowledge in the areas of tire geometry, dynamic tire behavior, chemistry of component materials, and technology of composite structures is essential [1]. Furthermore, due to the important role displayed by textile reinforcements in tire performance, there is a great need to study and understand the mechanical behavior and properties of these materials. The tensile test is perhaps the most important test to study the mechanical response of one material [15]. Often, tensile properties of one material are used to predict the behavior of a material under different forms of loading [16].

Digital image techniques have been used in textiles for a long time. With the technological development registered over the last decades in image acquisition, computer vision is becoming more affordable both as a research tool and as a process quality control [17]. The first objective of this project is to install a video camera on the dynamometer and to develop a test method to synchronize the video with the load-elongation curve. The second goal is to analyze and to study the images gathered, measuring the helix angle development along the tensile test.

In many ways, a tire is an engineering marvel. Geometrically, a tire is a torus. Mechanically, a tire is a flexible, high-pressure container. Structurally, a tire is a high-performance composite built using elastomers, fibers, steel, and a range of organic and inorganic chemicals. Tire technology is a complex combination of science and engineering that brings together a variety of disciplines [1]. And the result is a range of products which satisfy the needs for optimum performance under a wide variety of service conditions.

1.2 Work contributions

Improving tire's performance is an extremely challenging task. Constant research for better materials and technologies is necessary. The new and more advanced textile cord constructions, for tire reinforcement, build up the need to better understand and observe the textile cord morphological behavior. In order to obtain the load-elongation curve that characterize the textile reinforcements, normally tensile tests using a dynamometer are performed. Firstly, I incorporated a video recording setup in the available tensile machine. To enable the camera to follow the cord elongation, I conceptualized and designed an elevation device, which is currently being built. Finally, I used computer image analysis to measure and study the helix angle of the reinforcement cords tested. This will allow the acquisition of additional information about the mechanical and morphological characteristics of the tested samples.

1.3 Thesis organization

This document is organized in 7 chapters, which will be briefly described next:

1. **Introduction:** frames and briefly describes the problem. Also presents basic information about Continental and the tire industry and technology.
2. **State of the Art:** details the scientific knowledge on the subjects related, particularly on tires, textiles reinforcements, manufacture process and video analysis.
3. **Materials and Methods:** describes the procedures and methodology of the performed tests, as well as the materials used along the master thesis development.
4. **Results and Discussion:** presents and discusses the results achieved.
5. **Conclusions:** presents the conclusions established from the results obtained.
6. **Project Assessments:** gives a global appreciation about the developed work.
7. **References:** lists the bibliographic references that were used throughout the project.

2 State of the Art

The use of computer image analysis in the study of textiles is not groundbreaking. For that reason, comprehension of previous work done in this area is necessary for the development of this project. Besides, the reinforcement materials manufacture require a thorough process, which influence greatly the cord characteristics, and must also be contemplated.

2.1 Reinforcement materials

As in every subject, it is essential to understand and use unambiguous terms relating to textile reinforcing materials. The following terms and definitions are the necessary base to understand this project [18-21]:

Fiber - linear macromolecules oriented along the length of the fiber axis.

Filament - the smallest continuous component in a yarn.

Yarn - an assembly of filaments laid together.

Cord - a twisted structure composed of two or more yarns.

Linear density - defined as the weight of a specific length of cord or yarn. The most used unit is the decitex (dtex) and represents the weight in grams of length of 10,000 meters.

Twist level - the amount of 360° turns per unit length of a yarn or cord. Usually it is measured in turns per meter (tpm).

Breaking force - maximum force applied to a test specimen carried to rupture during a tensile test.

Tenacity - a measure of the tensile strength of a cord or yarn. It is defined by dividing the breaking strength by the linear density.

Load at specified elongation (LASE) - load applied to a cord for a specified elongation.

Modulus - slope of the initial linear portion of a force-elongation curve, expressed in newton per percentage.

Rubber is an elastomer with unique properties that make it an essential component of a pneumatic tire. It is soft, elastic, resistant to cutting and scraping, has a high coefficient of friction and low permeability to gases [22]. Many elastomers are too weak to be used without some reinforcing system. Either the elastomer matrix is compounded with reinforcing filler or the product is provided with some fiber consisting components applied in the product assembly phases [18]. As stated previously, both of them are used in tire production. Although, besides improving rubber's mechanical properties, fiber based reinforcements also provide adequate

functional properties to the product. Currently, five materials make up the major tire reinforcements usage: steel, rayon, nylon, polyester and aramid [3].

Fibers and steel cords are the primary reinforcement and load-carrying material in the tire. Thus, it is appropriate to review the properties to such materials for application in tires [1].

Carbon steel wire is used in tires due to its high strength and stiffness. Normally, the steel wire is coated with brass and was drawn, plated, twisted and wound into multiple-filament bundles. It is used in the belt ply and the bead core layers of the tire. These sorts of materials have the disadvantage of requiring special processing, having high weight and may suffer moisture corrosion [1, 3, 4].

Rayon is a fiber based on regenerated cellulose, and it was the first man-made fiber used in tire construction. The cellulose raw material can originate from cotton, or more usually, wood pulp [18]. The low-shrink, high-modulus, good-adhesion properties of rayon make it an excellent choice for use in passenger car tires. Rayon is more sensitive to moisture than the other fibers used in tire reinforcement [1, 18, 20].

Nylon is a polyamide polymer characterized by the presence of amide groups in the main polymer chain. Two nylon varieties are applied in tires: nylon 6 and nylon 6.6. They are most commonly used in radial tires as cap, belt edge cap strip material, and with some limited applications as body plies. Nylon provides reasonable strength, excellent adhesion and high fatigue strength [4, 23].

Polyethylene terephthalate (PET) is a polyester used widely in the synthetic fibers production. This polyester is strong, stiff, low-priced and provides excellent dimensional stability. On the other hand, it is not as heat resistant as rayon or nylon and requires a 2-stage dipping process compared to the 1-stage process used for nylon and rayon [20, 23].

Aramid is a synthetic, high tenacity aromatic polyamide fiber that is 2 to 3 times stronger than polyester and nylon. Characterized by a very high modulus and low elongation at break it can be used for belt or stabilizer ply material, as a light weight alternative to steel cord [4, 23].

All this fibers have distinct characteristics and mechanical behaviors. They are used in different layers with distinct functions, which grant the tires its unique features and attributes, and make it such a remarkable product. Yet, there can always be improvements, and finding new materials with unmatched characteristics is always an objective. One way of obtaining this is through hybrid cords, which are built with yarn of different materials twisted together. The outcome is a cord with unique mechanical properties, that could not be obtain from one single material. A schematic structure of a hybrid cord is presented in Figure 4.

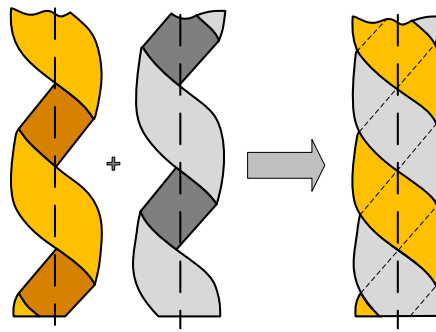


Figure 4 - Hybrid cord constitution (adapted from [19]).

The stress-strain curve of different materials used as reinforcement materials in tires is presented in Figure 5.

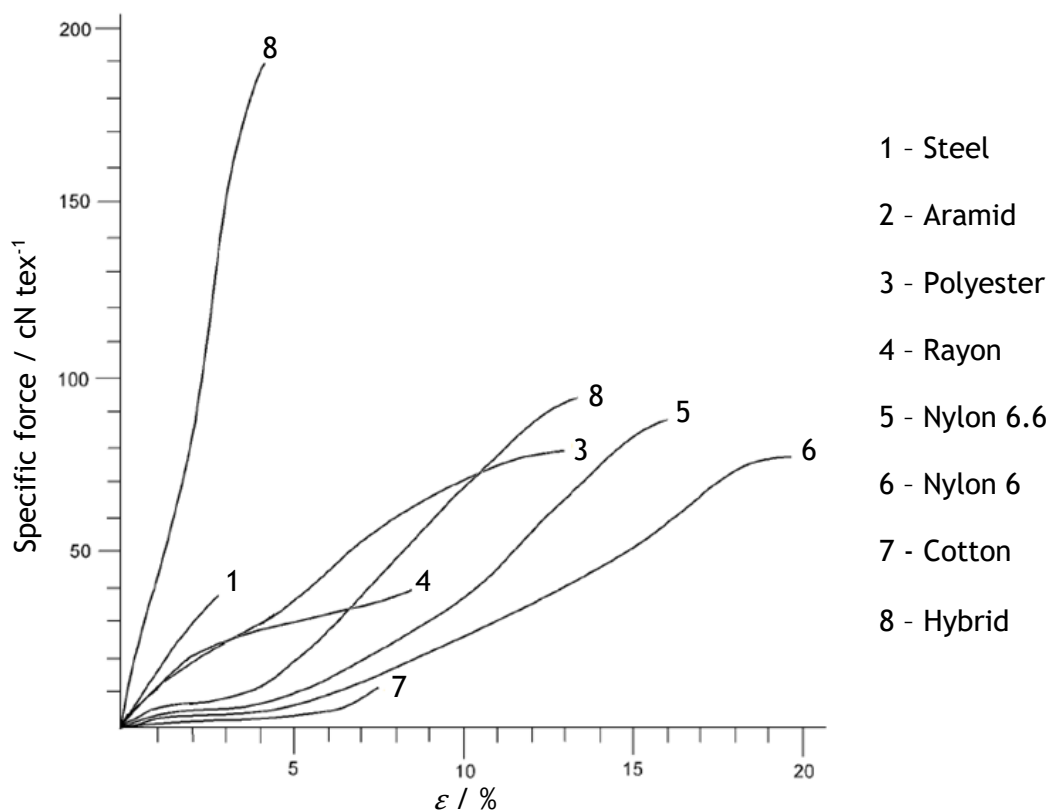


Figure 5 - Stress-strain curves of tire reinforcement materials (adapted from [20]).

2.2 Textile reinforcement manufacture

There are very few application where textile fibers can be used in the form in which they are originally produced. Usually, it is necessary to modify the yarn form or construction, in order to benefit from their incorporation as reinforcement in elastomeric composites [20].

The first step in textile reinforcement manufacture is the production of the filament. Filaments used in tire reinforcement are generally extruded through different spinning techniques, for example wet spinning, solvent spinning and melt/continuous spinning [24].

The spinning process of manmade fibers usually includes the following processes: Initially the preparation of polymer takes place (e.g. polymerization, chemical modification). Afterwards the spinning fluid (molten polymer or solution) is extruded through a spinneret. A drawing process follows, increasing the molecular orientation of the filaments and improving the tensile strength, modulus and elongation of the fibers. Finally, the filaments are heat treated and gathered, forming a yarn [25]. Although, yarn can also be made from staple fibers, which suffer an additional chopping stage in the spinning process.

2.2.1 Twisting

The twisting process is one of the most important processes in tire textiles reinforcement production, because twist level greatly influences tire cord performance [6]. Twist imparts durability and fatigue resistance to the cord, affects breaking elongation, breaking strength and the breaking mechanism [26]. Furthermore, without twist, the compressive forces applied to the cord would cause the outer filaments to buckle. A cord or yarn can be twisted in the “Z” and “S” directions, as displayed in Figure 6.



Figure 6- Twist directions (adapted from[19]).

The twisting process is normally accomplished in two stages. First, the yarn is twisted on itself to give a defined twist level in the “Z” direction, i.e., ply twisting. Afterwards, two or more spools of twisted yarn are twisted into a cord, in the “S” direction. A sketch of the twisting process is presented in Figure 7. The cord resulting from this process is designated greige cord.

If the yarn and cord are twisted in opposite directions with the same twist level, the cords are called balanced. Although, different cord characteristics can be achieved by other twist configurations. An unbalanced twist is defined by a different twist level on the cord and the yarn. Asymmetrical cords are the ones in which the yarns have different twist level between them.

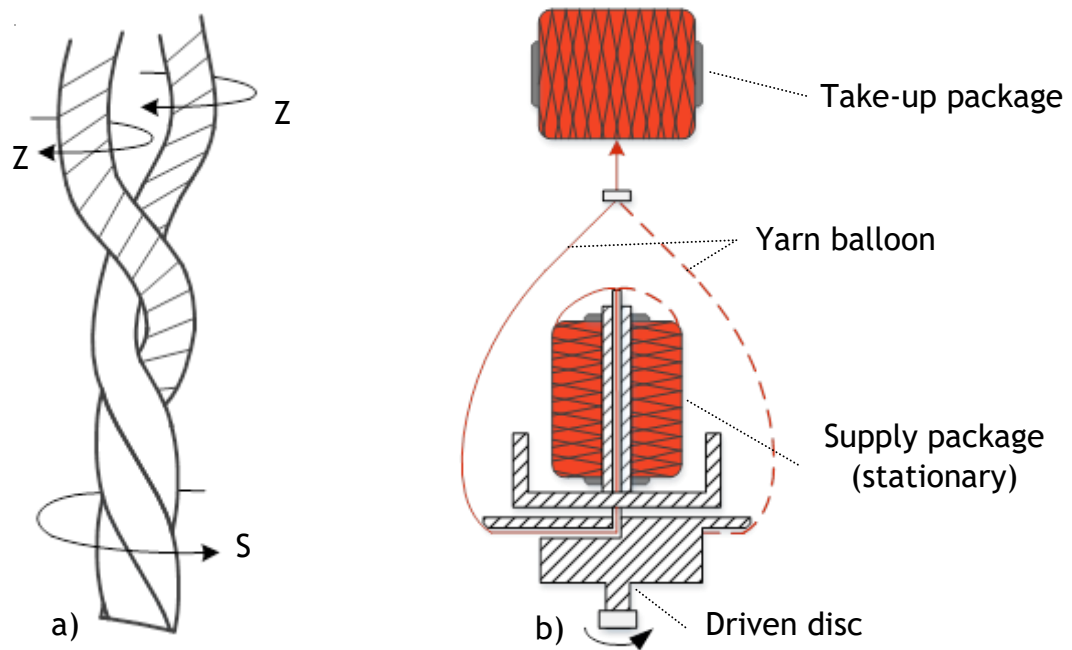


Figure 7 - Principles of twisting: a) twisting process (adapted from [19]) and b) twisting system (adapted from [20]).

The helix angle (α) is the angle formed between the cord axis and the yarn axis. As twist increases, the helix angle also increases (Figure 8). The study of the helix angle development along tensile test is one of the focus of the major focus of this project.

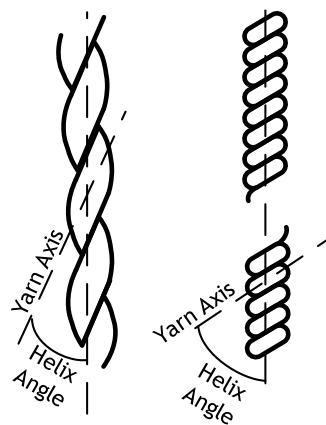


Figure 8 - Helix angle exemplification (adapted from [1]).

It is also necessary to better understand the mechanism of cord elongation. Elongation can be considered as structural and material elongation [19]. Higher twist level enlarge structural elongation, once the cord behaves like a spring, and the increase in maximum elongation is mostly due to the unfolding of the helix structure. Thus, tension stresses normal to the cord axis become greater, causing the filaments to break and the overall breaking strength to decrease [1, 13, 22]. When stretching a cord, a higher contribution of structural deformation

is noticed at the beginning. As the deformation progresses, material deformation becomes more preponderant.

2.2.2 Weaving

For tire reinforcements it can either be used single-end cords or cord fabric. For the production of fabric cord a weaving process takes place. A specific number of greige cords are laid lengthways (warp) and intertwined with the weft (that runs perpendicular) in a loom (Figure 9). The outcome is a very organized arrangement of reinforcement cords that can and be transferred to further operations [1].

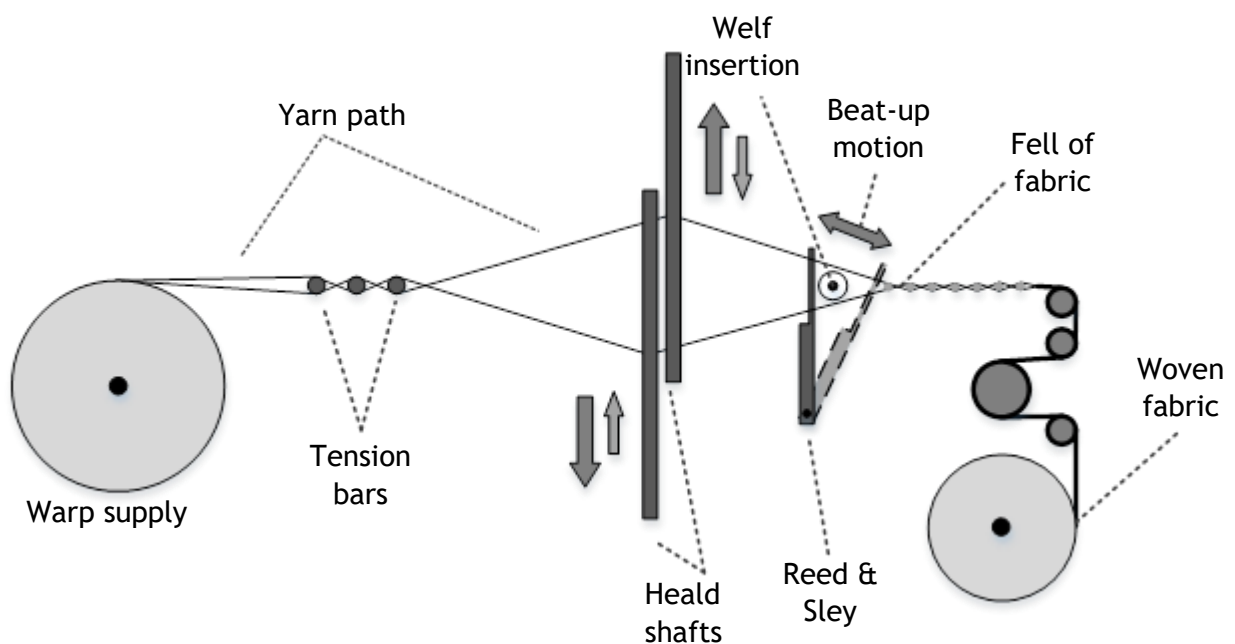


Figure 9 - Basic loom arrangement (adapted from [20]).

2.2.3 Dipping

The purpose of using textile cords for reinforcing rubber would not be met unless the composite matrix and the cords have considerable bonding forces. The dipping process has the objective of providing good adhesion properties to the cord or fabric. There are three aspects to adhesion of tire cord to the elastomer treatment: molecular, chemical, and mechanical. Molecular bonding is due to absorption of adhesive chemicals from the adhesive dip onto the fiber surface by diffusion. Chemical bonding is achieved through chemical reactions between the adhesive and the fabric and rubber, i.e., crosslinking and resin network formation. Mechanical adhesion is a function of the quality of coverage of the cord by the rubber coat compound. The greater the coverage, the better the adhesion [1]. For this purpose the cords pass through a resorcinol, formaldehyde and latex emulsion (RFL-dip) bath. Aramid and polyester are much less reactive

to standard RFL dip and must be pretreated with an isocyanate and polyepoxy pre-dip [21]. This process is represented in Figure 10.

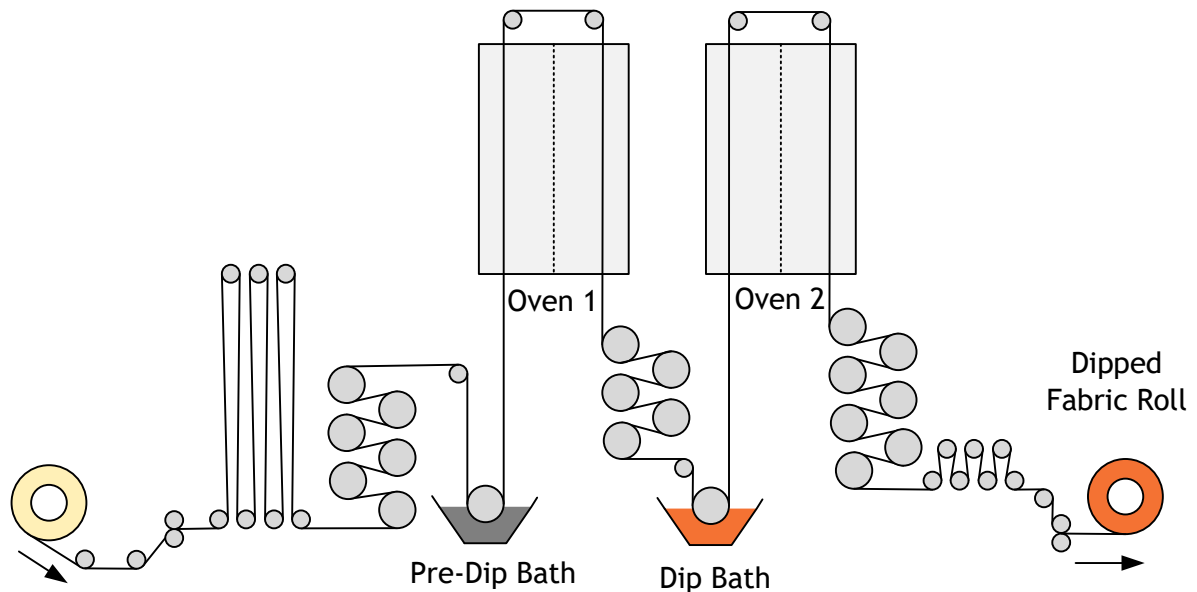


Figure 10 - Dipping and Heat treatment process (adapted from [20]).

To obtain optimum cord properties of strength, shrinkage, and modulus, specific temperatures and tensions are set at various exposure times within the dipping process unit. The temperature and tensions determine the ratio of crystalline and amorphous areas within the fiber as well as the orientation of the crystallites. These factors are determinative in the physical properties of the cord. Increasing processing temperature can decrease cord tensile strength and modulus but will improve fatigue performance. Stretching the cord in the first heating zone and then relax it in a controlled way in the second zone will regulate the cord shrinkage behavior [1, 6, 21].

The tensile strengths of the cords are slightly decreased in comparison to greige cords values. Dipping and treatment operations cause also reduction in the elongation at break values of dipped cords. For that reason, breaking energy of the dipped cords is lower than that of greige cords [6].

The result of this production stage are high performance dipped cords or fabrics that can move forward to further processing. Following, the reinforcement materials are calendared, where the reinforcements are pressed against a rubber compound by two rotating rolls.

In Figure 11, dipped cords with different twist levels, resulting from the dipping process, are represented.

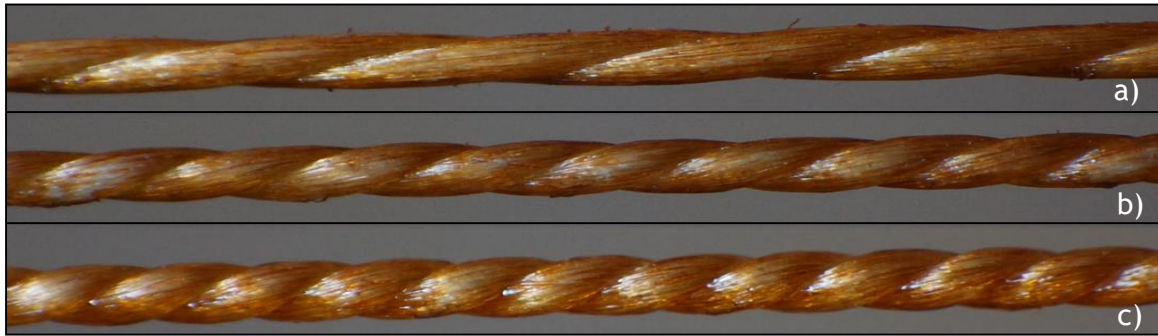


Figure 11 - Textile cords with different twist levels (a) 200 tpm, (b) 400 tpm, and (c) 550 tpm.

2.3 Video analysis

A video is a series of photographs captured from the surrounding environment, giving information about the changes in the registered object. In modern video cameras, the light enters the camera through a set of lenses and hit a charged-couple device (CCD) with a set frequency. A CCD is a lightsensitive integrated circuit that stores irradiated image data in such a way that each acquired pixel is converted into an electrical charge [27]. The information is afterwards processed and recorded. The video camera mechanism is presented in Figure 12.

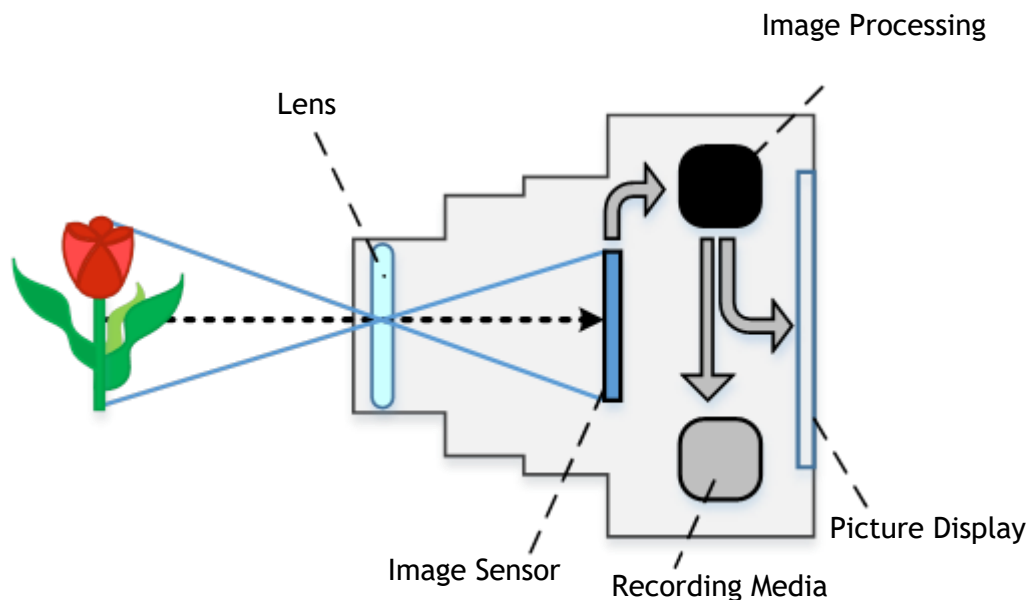


Figure 12 - Digital camera mechanism (adapted from [28]).

It is of extreme importance to consider some parameters in image acquisition devices, such as focal length, image resolution, shutter speed and frame rate. Focal length is a measure of how strongly the system converges or diverges light, affecting the distance in which the camera can focus an object. The image resolution concerns the detail an image holds, in which higher resolutions means more image detail. The shutter speed, as the name says, is the time that a

shutter allows the light to hit the CCD and the frame rate defines the number of images taken per time unit, usually measured in frames per second (fps).

When recording moving objects one must consider that it takes time to acquire an image. If the displacement in the recorded object is too high while the shutter is open the result will be a blurry image, despite of the resolution of the camera. High-speed cameras are remarkable due to its capacity of high frame rate capture (up to more than 100 000 fps) which in this case demands also an incredible small shutter speed. One must also consider that the area of interest must be defined accordingly to the camera resolution. If it is intended to film an object with great description, the area recorded must not be too large, in order to keep a high amount of pixels per length recorded.

Modern digital technology has made it possible to manipulate image in order to acquire further information from recorded objects and phenomena. Categories of image manipulation include: image analysis, that is the process of making measurements from this images, and image understanding, the achievement of high-level descriptions from images [29].

For a long time, digital image techniques have been used in textiles, mostly for examining and analyzing the structural parameters of yarns like hairiness, irregularity, number of twists and yarn appearance [17]. Currently, several systems to visualize yarn and fabric qualities are available. Several types of images are created directly from yarn profiles captured from measurement systems. These systems are not completely satisfactory due to the lack of quantitative measure, once the images are often judged visually [17].

The need of a test method that enables test recording and further analysis was long felt [30]. This project focus on the development of a test method that enables image analysis and understanding of textile cords morphological behavior, specifically the measurement of helix angle development in tensile test.

3 Materials and Methods

In this chapter the equipment, techniques and methodologies used in the development of this project will be described.

3.1 Equipment

3.1.1 Video recording equipment

For the development of this project, three different cameras (Figure 13) with different characteristics were used.

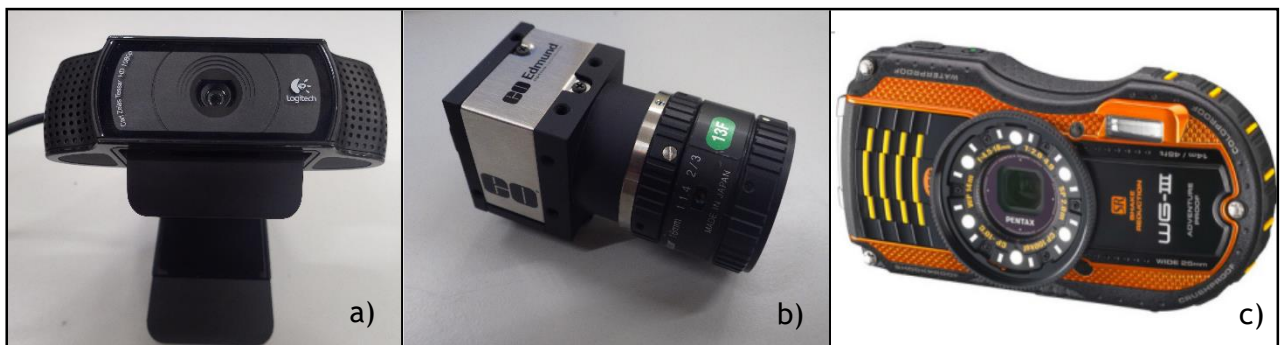


Figure 13 - Different cameras used in the development of the test method: a) Logitech, b) EdmundOptics and c) Pentax WG-III.

Controlling light surrounding condition is also an issue in image acquisition setups. For that, artificial illumination sources are used. Led lights are preferred over regular fluorescent lights, once have a more continuous light emission. Using florescent lights when recording at considerable high frame rates leads to flickering problems. The illumination sources tested are presented in Figure 14.



Figure 14 - Artificial light sources used: a) led flashlight and b) led spotlight.

In the USB digital cameras, the automatic synchronization between the video and the load-elongation curve is possible. For that, a laser beam was used. The laser is pointed to the

background and it turns on when the test starts. As soon as the pre-tension has been applied to the cord, the laser shuts off, marking the beginning of the load-elongation curve.

Other material as tripods and backgrounds were also used in the test method development.

3.1.2 Laboratory twisting unit

Helix angle, as stated before, is directly linked with twist level. For that reason cords with different twist levels were built.

Several two yarn balanced polyester cord were twisted with different twist levels in the Laboratory Twisting Unit (LTU), depicted in Figure 15. This machine has the same twisting method than the ones used in industrial production. In the first step, the yarn is twisted on itself in the “Z” direction and afterwards the yarns are twisted together in the “S” direction with the same twist level. A length of 1 000 meter of each cord was twisted.



Figure 15 - Laboratory Twisting Unit.

3.1.3 Twist tester

The twist tester is an equipment used to measure the cord twist level (in turns per meter). The tests were performed accordingly to the ASTM D885M. In this project a Zweigle twist tester was used (Figure 16).



Figure 16 - Zweigle twist tester.

3.1.4 Laboratory dipping unit

The laboratory dipping unit (LDU) is a scaled-down dipping machine. It allows the study of process parameters and without interfering with the industrial production process. This machine, represented in Figure 17, was used during this project to study the influence of the dipping process in the cord helix angle.



Figure 17 - Laboratory Dipping Unit.

Only polyester cords were impregnated in the LDU, consequently a pre-dip and a dip were necessary. The greige cord is dipped in the 1st bath (pre-dip) and follows to the 1st dry zone. It

is dried and stretched before being dipped in the 2nd bath. The cord is again dried and relaxed, being finally wound up in a spool. The cord residence time in each zone is controlled by the speed and number of passages through that zone. The stretch level is controlled by the difference of rotating speed of the rolls before and after each oven.

3.1.5 Tensile machine

The Zwick Roell tensile test machine, represented in Figure 18, was the main test machine in this project development. The cord is attached in-between the two clamps. When the test starts the superior arm moves, making the superior clamp to move along and therefore the cord to be deformed. A load cell is located in the middle of the superior arm and the clamp, registering the load exerted by the cord along the test. The normal tensile test is position controlled, since there is a defined displacement speed throughout the test. Load controlled tests are also possible, using a PID control system, adjusting the displacement speed to assure linear increase in the load applied.

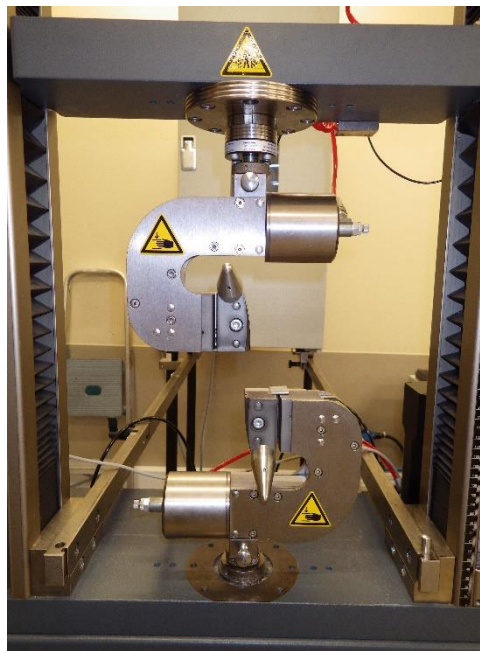


Figure 18 - Zwick Roell tensile test machine.

3.2 Technical procedure and conditions

Cords with different twists level were dipped in order to study the morphological change caused by the dipping process. The LDU condition used in the process are presented in table 1. The net stretch of the overall process was 1.5 %, and were used standard dip and pre-dip solutions.

Table 1 - Dipping conditions used in LDU.

Zone	Temperature / °C	Exposure time / s	Stretch level / %
1st dry	160	64.3	0.9
Hot stretch	235	45.9	2.9
2nd dry	135	27.6	-2.3
Normalizing	235	45.9	0.0

To obtain the load-elongation curves the ASTM D885 was followed. [31] The tests were performed at room temperature (23 ± 2 °C) at a displacement speed of 300 mm min^{-1} . The superior clamp moves at the test speed while the lower clamp stands still (Figure 19). The length of each sample tested was 250 mm. At least, a cord should be tested 5 times. Before the test begins, the cord should be strained by applying a pre-tension (σ_0 in N) resulting in multiplying the cord linear density in dtex by a 0.05 factor.

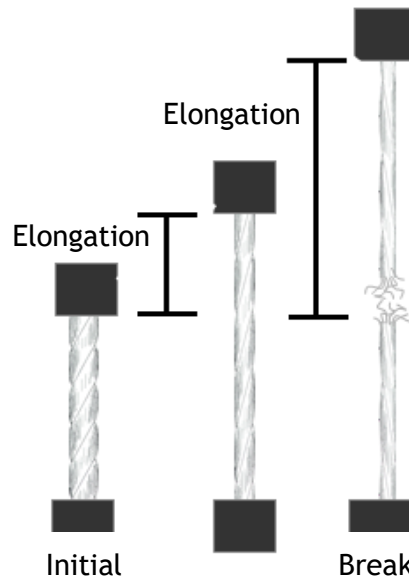


Figure 19 - Load-elongation test (adapted from [19]).

When characterizing a cord behavior, one of the most important test is the mechanical hysteresis. It is the test that best resemble the actual tire cord behavior, suffering several cycles of load. The test was made accordingly to internal procedure.

For this test 50 load-unload cycles between 2 % and 4 % elongation were performed at room temperature, using parallel clamps. The load-elongation curve of the mechanical hysteresis was measured.

4 Results and Discussion

In this chapter the entire process towards the test method development, from the installation setup to the results and possible applications will be presented and discussed.

4.1 Installation setup

The first step in the test method development was to test the equipment available and define the adequate installation setup. As stated before, three cameras were available for testing. To proceed to further image analysis a good quality image has to be gathered. The EdmundOptics camera can only register 7 fps, which results in a blurry image where the helix cannot be distinguished. The Logitech camera is capable of capturing at 15 fps if the resolution is 960x720 pixels. Finally, the Pentax WG-III camera records at a frame rate of 30 fps with a resolution of 1920x1080 pixels, consequently it was the camera selected to perform the tests. It is also required to notice that in order to have a sufficient clear image to analyze, the area of interest had to be narrowed down to a cord length of 2 to 5 cm. This means that only a portion of the cord is recorded during the test. The difference between the images gathered with the different cameras is present in Figure 20.

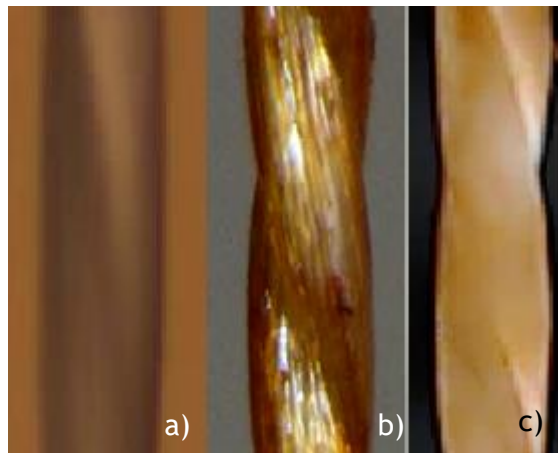


Figure 20 - Images obtained with different cameras: a) EdmundOptics, b) Pentax WG-III and c) Logitech.

Without the proper recording conditions, the camera characteristics become almost irrelevant once one cannot record correctly the intended object. Illumination conditions are one of the most significant parameters in video recording. Having a totally controlled illumination is the best option, although it was not possible in this case, since the Zwick machine is placed in the same laboratory as other equipment that must be used at the same time. The solution found was to point a light source at an oblique angle in order to enhance the cord helixes, and make the posterior analysis easier and more accurate. Illumination too intense will overcome the

cord contours and make the helix indistinguishable. For that reason only the led flashlight was used, being the led spotlight excluded. The influence of proper illumination is represented in Figure 21. Besides illumination conditions, the use of a white background was found convenient, although it has a smaller influence in the quality of the image and the helix angle analysis.

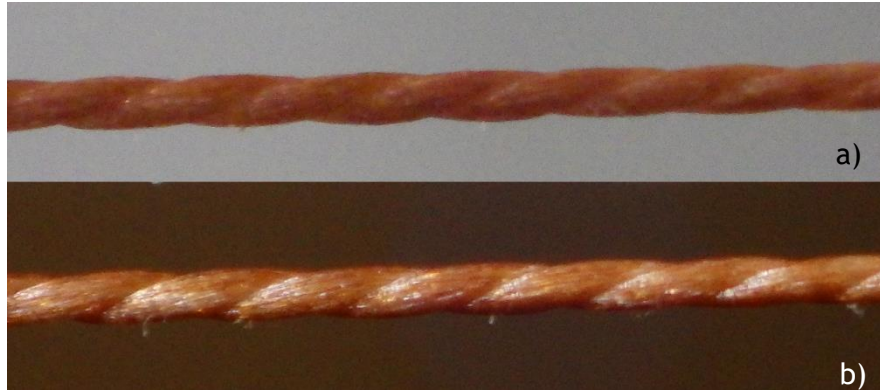


Figure 21 - Influence of proper illumination enhancement: a) without controlled illumination and b) with controlled illumination.

The Zwick machine is equipped with a test interface, textXpert [32]. This interface is responsible for processing the data generated in the tensile test, presenting the results and respective statistical analysis. It was possible to program the software to automatically synchronize the recorded video with the load-elongation curves. For that purpose a laser beam was pointed towards the sample background. Once the operator starts the test the laser turns on until the cord pre-tension is applied. When the pre-tension is reached the laser turns off. The software detects the change in the background and synchronizes the beginning of the video with the load-elongation curve. This is only possible with USB connected cameras, which is not the case of the Pentax WG-III. Although, since this software is not capable of further image analysis (e.g. helix angle measurement) another software was required, discarding the biggest advantage of automatic synchronization.

For the image analyses and helix angle measurement the following software were tested: PhysMO [33], ImageJ [34]; Icy [35] and Tracker [36]. Tracker was the chosen interface due to its user-friendly interface, extensive analysis and measurement tools, and easy data exportation process. The software works through frame-by-frame analysis of the video sample. In order to synchronize the video with the load-elongation curve the frame where the cord breaks is registered as the maximum load point. The test duration is then accounted in the video and the test start frame is also registered. Alternatively, as the pre-tension speed is extremely low relatively to the test speed, the moment the cord starts to elongate is visible by frame-to-frame comparison. For the helix angle measurement a protractor tool was used. The Tracker software user interface is presented in Figure 22.

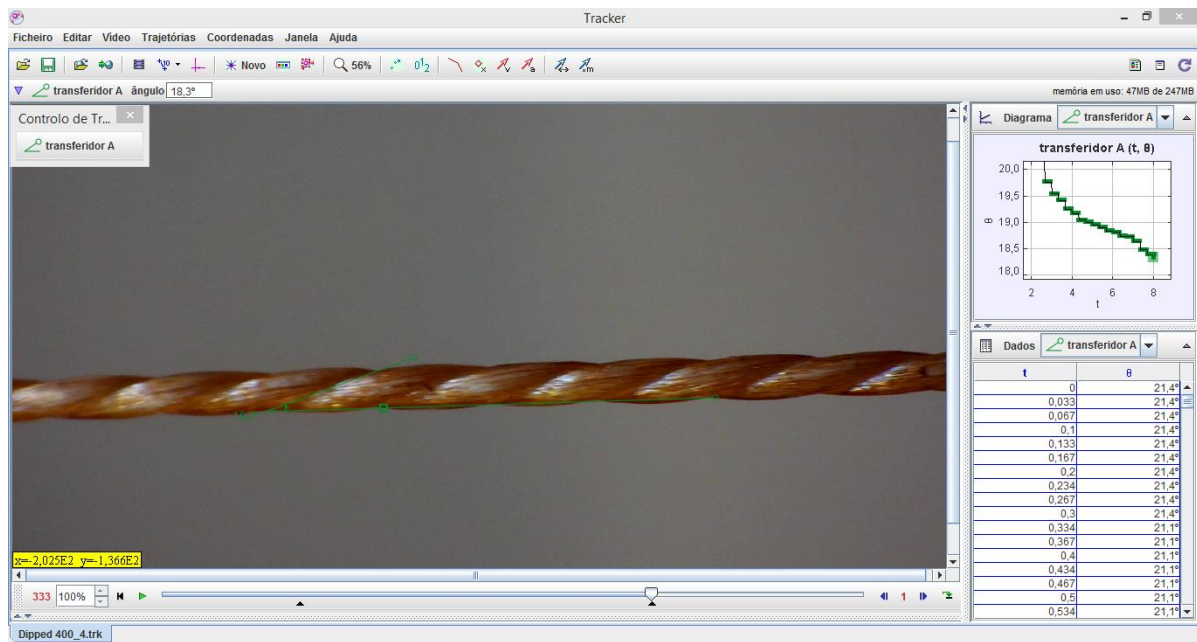


Figure 22 - Tracker software user interface.

The determination of the best test method procedure was a time consuming process that resulted in the set up presented in Figure 23. When performing the tests, one must be concerned if the video camera is set perpendicularly to the cord sample. Otherwise the distance between the camera and the sample will change during the test, causing the image to become out of focus. This can be controlled by the tripod level indicator.

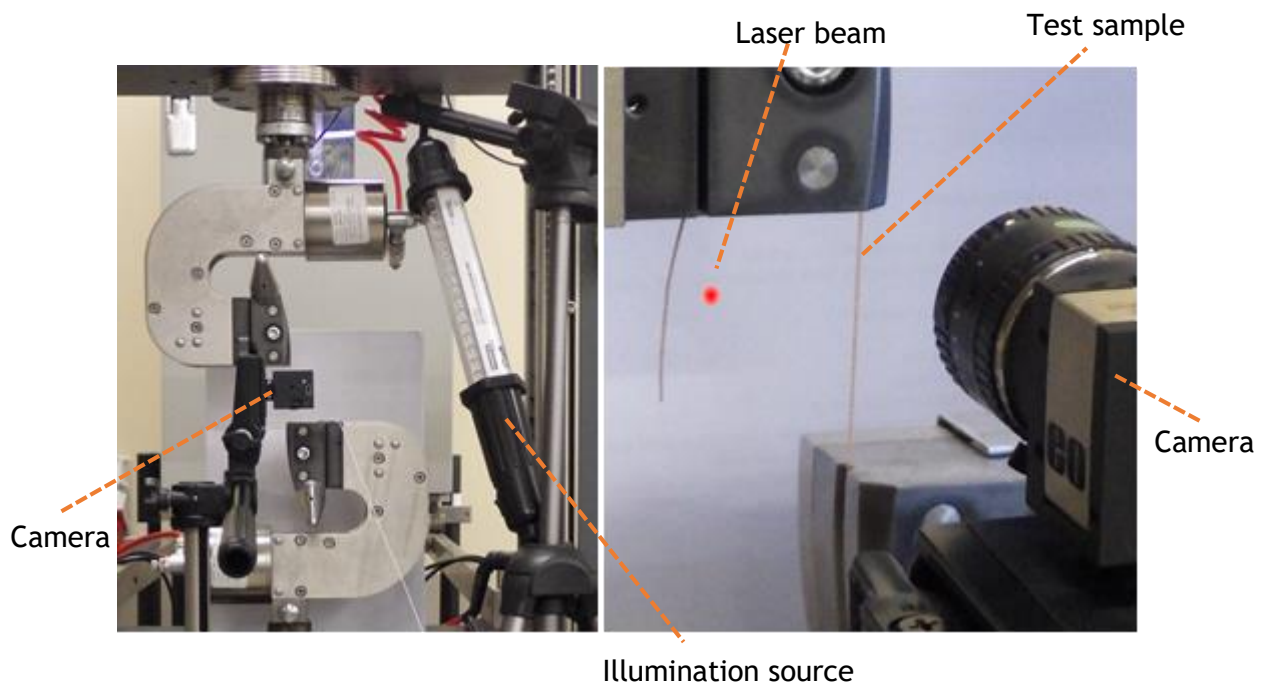


Figure 23 - Installation setup of the test method.

4.2 Image analysis setup

Regarding the test performed for the set up development, standard Nylon and Polyester cord with medium twist level were used. The first problem that arose was the uncertainty in the helix angle measurement. In order to make the process accurate and uniform for all cords tested a few considerations had to be done. The protractor tool used is composed of two adjustable lines that create an angle. One of the lines is placed along the cord axis and the other in the yarn axis. It is crucial to notice that the helixes are not straight lines. All things considered, the helix angle is measured by placing the protractor vertex above the point where one yarn overcomes the other and placing one line over the similar cord axis points and the other line in the yarn axis. In Figure 24 these considerations are outlined and the actual measured helix angle (θ) displayed.

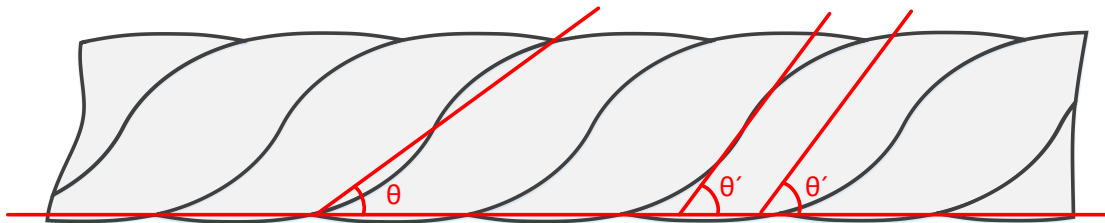


Figure 24 - Measured helix angle (θ) disambiguation.

Textile cords are not perfectly twisted homogeneous structures. They present differences in the twist level along the cord, and consequently lengthwise variations of the helix angle. Since one of the goals of this project is the study of helix angle evolution along force-elongation tests, a representative value of the helix angle is required. The actual camera can record ca. 5 cm of the cord, which is not sufficient to cover the whole length during the test. Two approaches were then devised for addressing this challenge. The first solution, was to develop an elevation device that allow the camera to follow the cord elongation while keeping the same portion of the cord inside the recorded area. A prototype was created of this purpose using SolidWorks [37], and is represented is Figure 25.

The second solution, was to keep the camera stationary and make an average of three consecutive helix angle values. To be able to compare the results obtained in different cords, the same position of the cord, relatively to the clamps, has to be recorded in all tests. The position of the camera was controlled in the tripod.

The complete test procedure is described in the Attachment I.

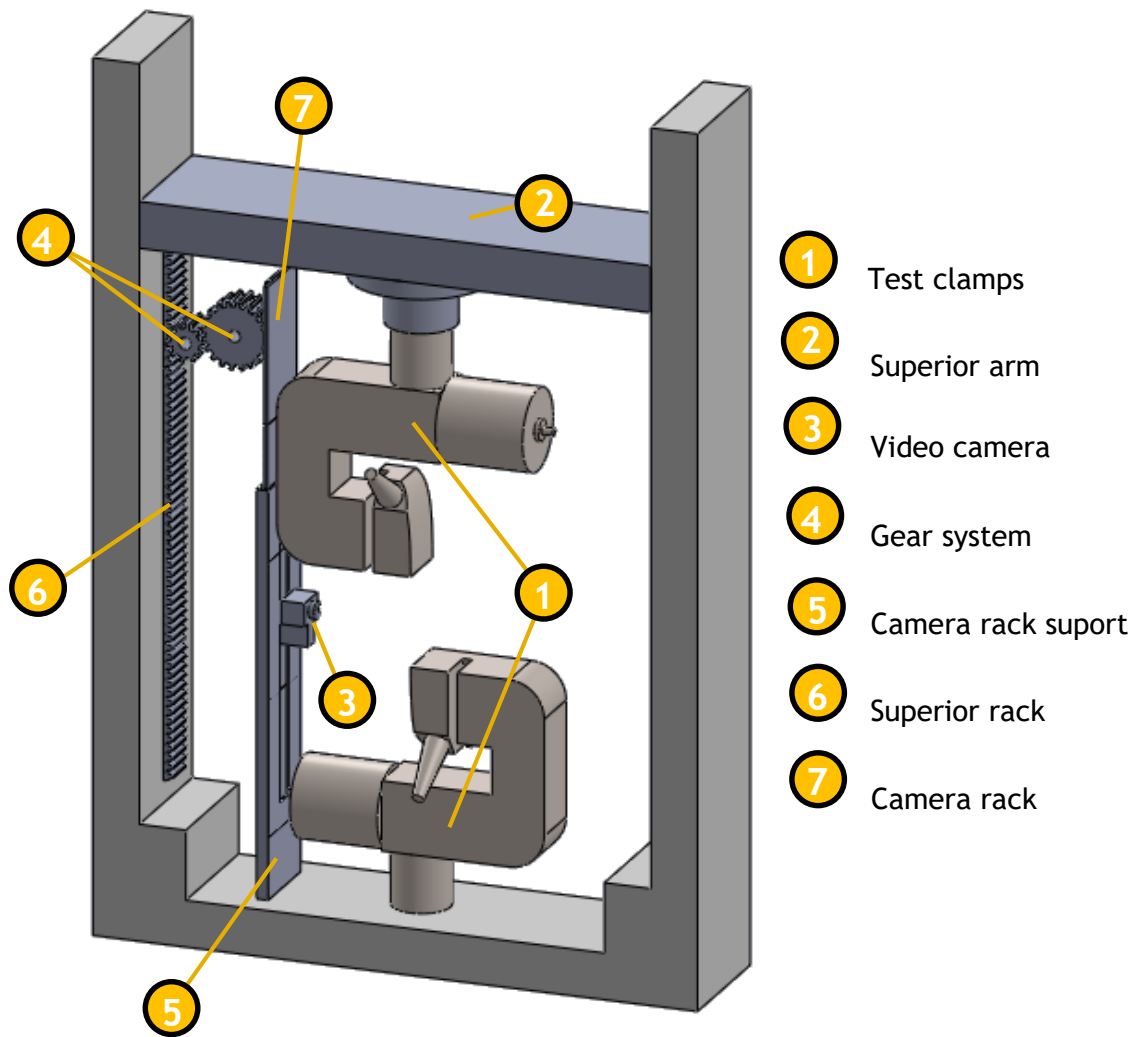


Figure 25 - Zwick elevation device.

The device is a quite simple working mechanism. The Superior rack is attached to the Superior arm, which rises during the test. Connected to it, a set of two gear with different gear ratio impart the Camera rack half the speed of the Superior Rack. The Camera rack slides through a fixed support, making the Camera move along the cord at half speed relatively to the superior arm. The front view of the device in the beginning and end of the test is sketched in Figure 26.

The described elevation device was projected to work for different cameras and is currently being built in C-ITA. Although, it was not ready in time to be used in this project, and the second approach had to be used in the performed tests.

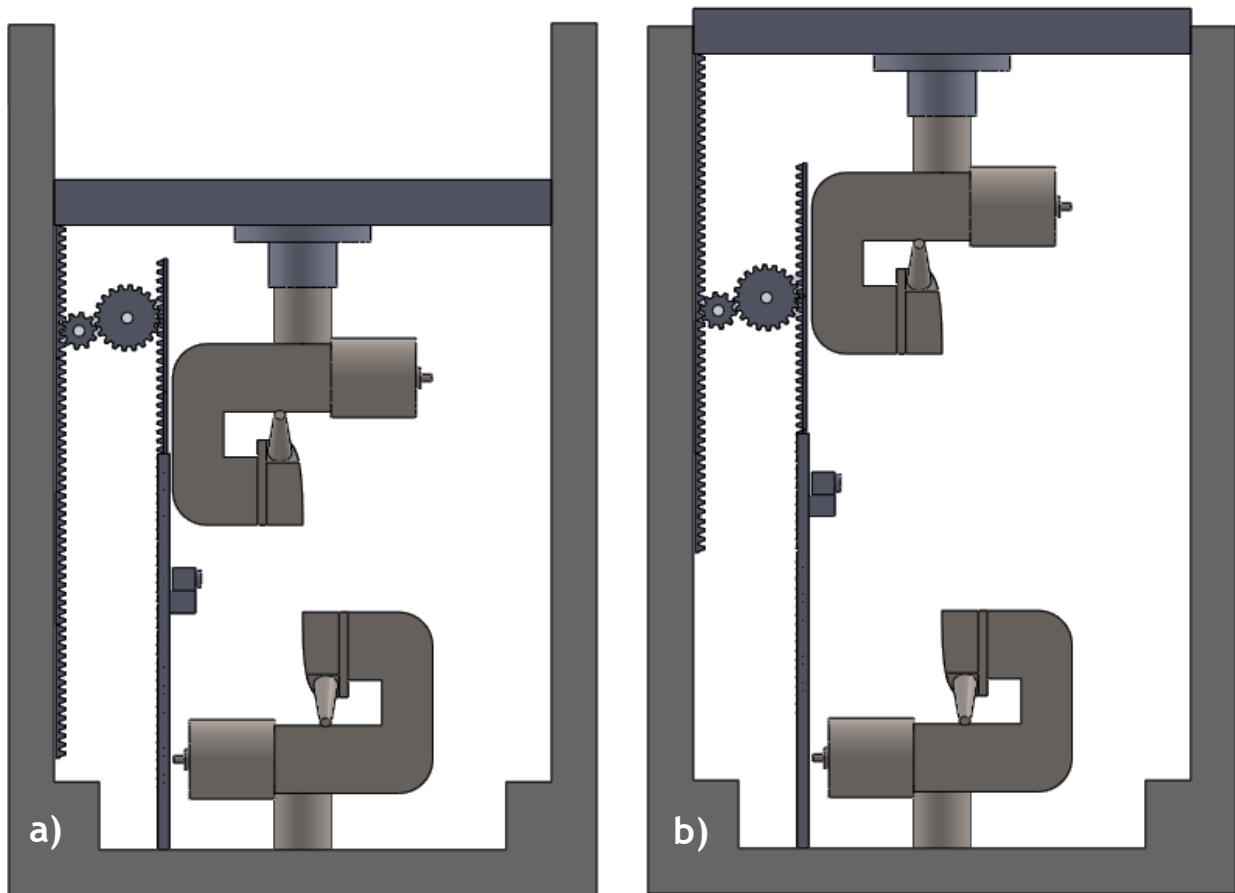


Figure 26 - Zwick elevation device: a) test beginning and b) test end.

Before carrying any further studies about the test method applications, the repeatability and the influence of the operator in the image analysis procedure was tested. The reproducibility is defined as the closeness of agreement between the results of successive measurements of the same measurand carried out subject to the same measurement procedure, the same observer and repeated over a short period of time [38]. Using the same operator, 50 measurements of the helix angle in the same image were carried out in greige and dipped PET cords. The results are summarized in Table 2.

Table 2 - Repeatability of the image analysis.

Dipped Cord		Greige Cord	
Average $a / ^\circ$	$s / ^\circ$	Average $a / ^\circ$	$s / ^\circ$
20.22	0.13	18.62	0.19

From the results obtain, we can conclude that the standard deviation in the measurements is bigger in the greige cord than in the dipped one. This is due to the fact that the greige cords

are more irregular causing more variations in the cord and yarn axis determination, therefore in the helix angle. Although, in both cases, the value is minor comparatively to the angle value.

To study the operator influence on the helix angle was measured by 5 different operators in greige and dipped PET cords. In each cord 6 values were measured, being the results represented in Table 3 and Table 4.

Table 3 - Operator influence on helix angle measurement in greige cords.

Greige						
Operator	A	B	C	D	E	s / °
Sample 1	17.6	17.3	17.8	17.4	17.9	0.23
Sample 2	17.3	17.4	17.5	17.3	17.6	0.12
Sample 3	16.6	16.3	16.0	16.4	16.6	0.24
Sample 4	16.3	16.2	16.5	16.8	16.5	0.21
Sample 5	13.8	13.9	14.0	14.1	13.7	0.14
Sample 6	13.8	13.8	14.2	13.9	14.3	0.21

Table 4 - Operator influence on helix angle measurement in dipped cords.

Dipped						
Operator	A	B	C	D	E	s / °
Sample 1	30.3	30.8	30.1	30.2	30.3	0.24
Sample 2	30.5	30.3	30.6	30.1	30.2	0.19
Sample 3	27.2	27.7	27.1	27.4	27.7	0.25
Sample 4	27.6	27.6	27.5	27.8	27.7	0.10
Sample 5	25.5	25.1	25.4	25.0	25.2	0.19
Sample 6	26.2	26.2	26.6	26.4	26.6	0.18

The standard deviation of the measurements among operators is in all cases equal or smaller than 0.25°. The measurements differ always less than 2 % of the helix angle value, which can be considered a consistent result that validates the use of this analysis to determine the helix angle of textile cords.

4.3 Test method application

Once the test method is established, it is now time to present and discuss its applications in the study of textile reinforcement materials. For this study, different cords were build and tested so the results may work as proof of method.

Greige Cords

The first study performed is concerned by the influence of twist level on the helix angle. Using 1440 dtex PET yarn, balanced cords with different twist level were built. The different cords tested are presented in Table 2. The greige cords were built in the LTU, except the cord with 560 tpm, 580 tpm and 600 tpm, which had to be twisted in the Production Twisting Unit since the LTU cannot produce such high twist levels. The twist level was afterwards measured in the Zweigle twist test. All the cords have an average measured twist level of ± 5 tpm from the desired value.

As the elevation device was not ready, the average of three consecutive helixes in the same cord were considered representative. It was considered that the cord was faulty if the standard deviation of the measured angles was above 0.5° . This presents the first advantage of the test method, once it allows to evaluate the regularity of one cord lengthwise. For each twist level were tested five different cords at the pre-tension, breaking moment, LASE 2 % and LASE 4 %. The results are described in Table 5.

Table 5 - Twist level influence in the helix angle in greige cords.

Cord	Pre-tension		LASE 2 %		LASE 4 %		Breaking		Maximum Load		Maximum Elongation	
Twist / tpm	$\alpha / ^\circ$	$s / ^\circ$	$\alpha / ^\circ$	$s / ^\circ$	$\alpha / ^\circ$	$s / ^\circ$	$\alpha / ^\circ$	$s / ^\circ$	Load / N	s / N	$\varepsilon / \%$	$s / \%$
100	6.56	0.22	5.94	0.32	5.81	0.40	4.54	0.33	224.17	3.18	12.69	0.43
120	8.57	0.48	7.26	0.41	6.41	0.39	5.59	0.30	227.46	1.28	13.50	0.13
140	8.94	0.50	7.80	0.49	6.72	0.41	5.89	0.17	228.05	1.05	13.69	0.19
180	11.21	0.45	9.75	0.38	8.86	0.50	7.54	0.43	230.26	1.67	14.38	0.16
200	12.67	0.44	11.02	0.32	10.37	0.23	9.04	0.13	222.65	1.24	14.28	0.33
220	13.15	0.28	12.21	0.31	10.89	0.47	9.69	0.24	221.48	3.09	14.47	0.31
280	16.25	0.48	15.30	0.18	14.46	0.08	11.26	0.36	225.17	1.48	15.59	0.30
300	18.27	0.43	16.67	0.41	15.61	0.49	11.68	0.42	223.37	2.15	15.89	0.38
320	18.98	0.36	17.61	0.37	16.21	0.38	12.28	0.43	223.39	2.53	16.19	0.50
380	23.52	0.34	21.51	0.44	19.46	0.43	16.72	0.36	216.78	1.83	17.57	0.38
400	25.18	0.40	23.22	0.35	21.20	0.35	18.09	0.38	207.09	2.91	17.66	0.53
420	26.51	0.10	23.69	0.34	22.40	0.23	18.53	0.34	206.32	6.63	18.02	0.90
480	28.55	0.50	25.23	0.41	23.75	0.40	20.58	0.41	196.14	8.10	18.42	0.73
500	29.12	0.24	26.22	0.20	25.10	0.17	21.42	0.29	192.63	7.63	18.71	0.57
520	29.69	0.37	27.64	0.22	26.67	0.30	21.31	0.56	186.61	3.33	19.24	0.39
560	32.31	0.50	29.97	0.34	28.97	0.32	23.59	0.33	179.07	7.02	19.66	0.68
580	33.46	0.08	31.43	0.27	29.58	0.32	23.81	0.18	172.57	5.07	19.96	0.37
600	35.36	0.27	32.80	0.30	30.41	0.49	25.25	0.32	170.03	4.21	21.08	0.52

The goal of building cords with these specific twist levels was at first to have 100 tpm apart from each one. The tire cord specification, once it is produced, indicate that twist level may vary by ± 20 tpm. Additionally, cords in that range were also build, except for the cords with 80 tpm and 620 tpm, which were replaced by 140 tpm and 560 tpm respectively, once they are out of the twisting machine capability.

A conclusion one can already make is, that in all situations studied, the helix angle increase as the twist level also increase. Is also notable that the biggest standard deviation values are slightly higher than 0.5° . For better understanding of these results, the variation of the helix angle with the twist level in each case is presented in Figures 27, 28, 29 and 30.

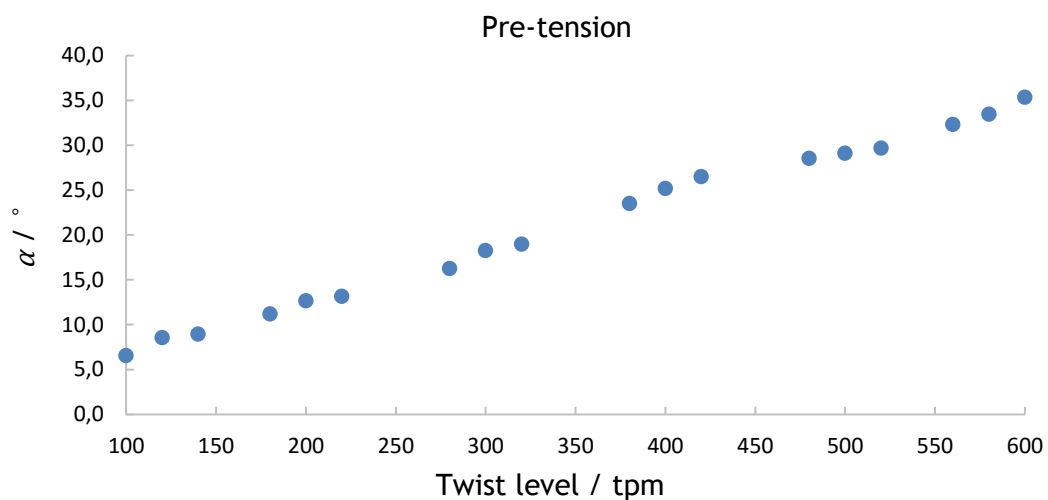


Figure 27 - Helix angle vs Twist level at pre-tension.

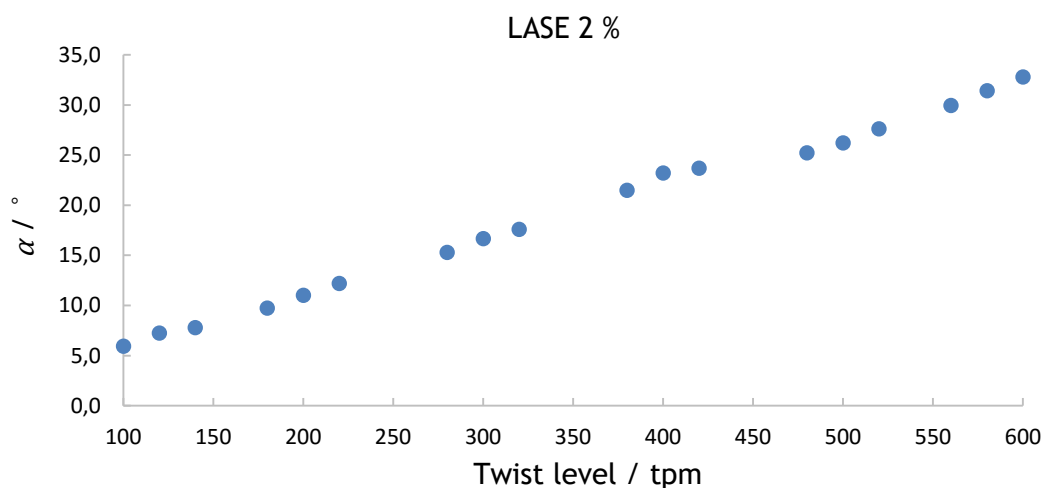


Figure 28 - Helix angle vs Twist level at LASE 2 %.

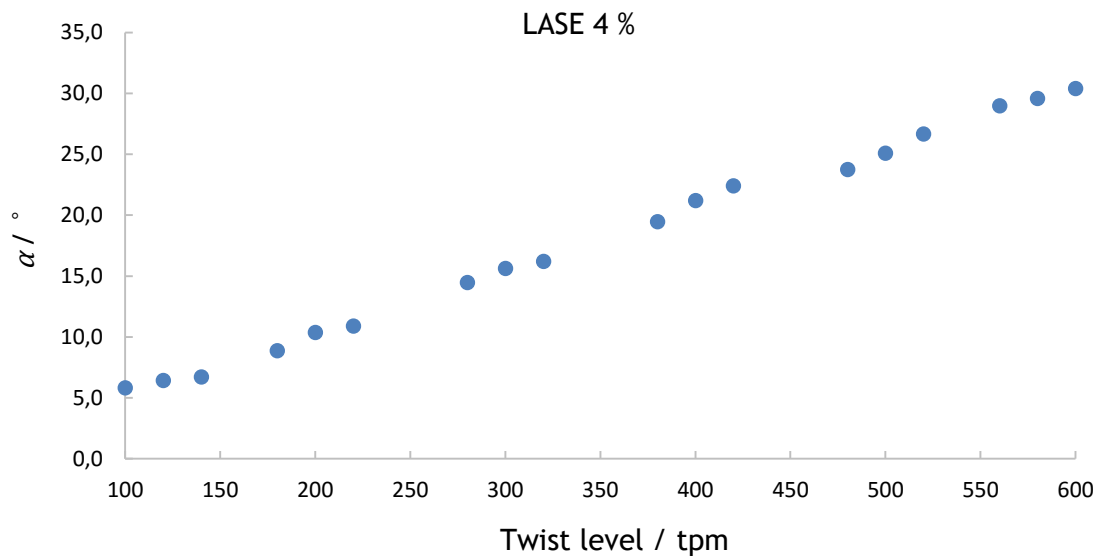


Figure 29 - Helix angle vs Twist level at LASE 4 %.

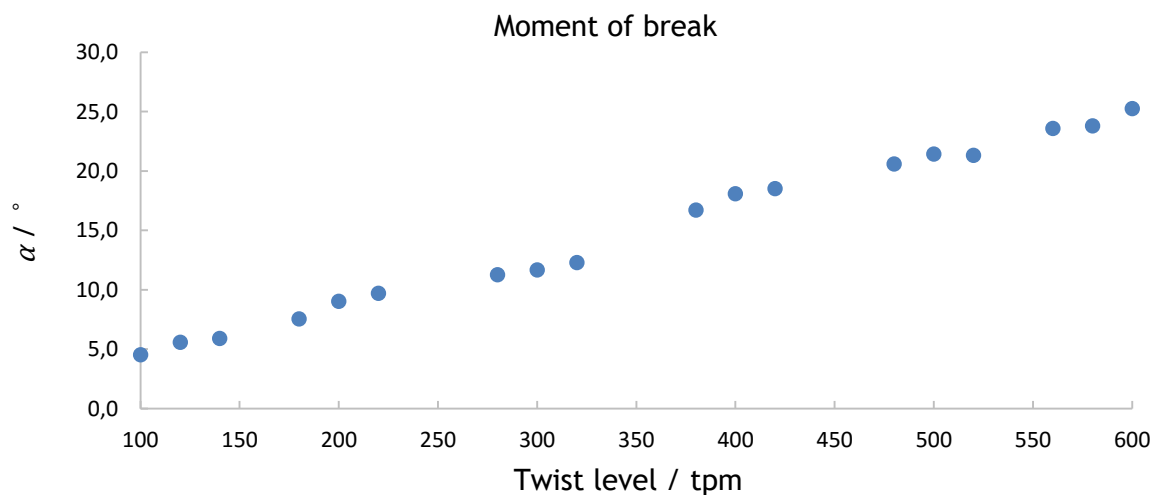


Figure 30 - Helix angle vs Twist level at the moment of break.

In all the cases, the helix angle increase as the twist level increases. Also, the amount of variation of the helix angle increase as the twist level increase, indicating a higher morphological mobility of the cords with higher twist levels.

The average load-elongation curves from some representative twist levels are presented in Figure 31.

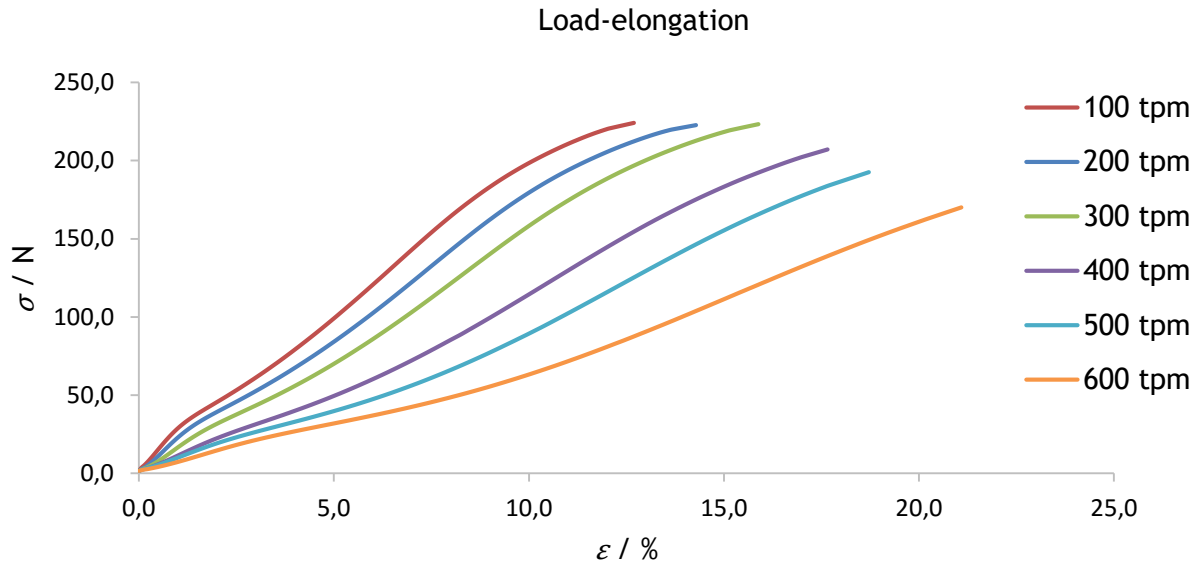


Figure 31 - Load-elongation curves of cords with different twist level.

As predicted, as the twist level increase the maximum elongation of the cords also increase, whereas the maximum load decreases. This observation is justified by the fact that as twist level increases the cord gains structural deformation capacity, reaching larger elongations. This also causes the friction forces between yarns to more preponderant, increasing the tension normal to the cord axis, causing the cord require less load to reach a breaking point.

This type of analysis is the standard for this test method, it includes important information about the morphological characteristics of the cord and demands a reasonable amount of time. Other points can be studied instead, as the helix angle at a specific load.

Further helix angle analysis is also possible. The variation profile of the helix angle along the test was determined by measuring the helix angle with a step of 10 frames, which means, a third of a second apart. The result obtained for PET greige cords with twist levels of 200 tpm, 400 tpm and 550 tpm are presented in Figure 32, 33 and 34 respectively.

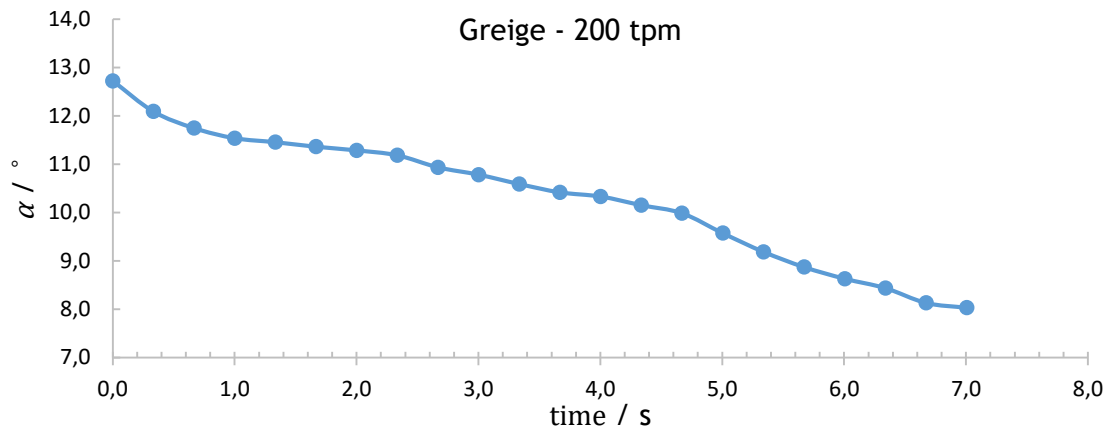


Figure 32 - Helix angle profile for greige 200 tpm cord.

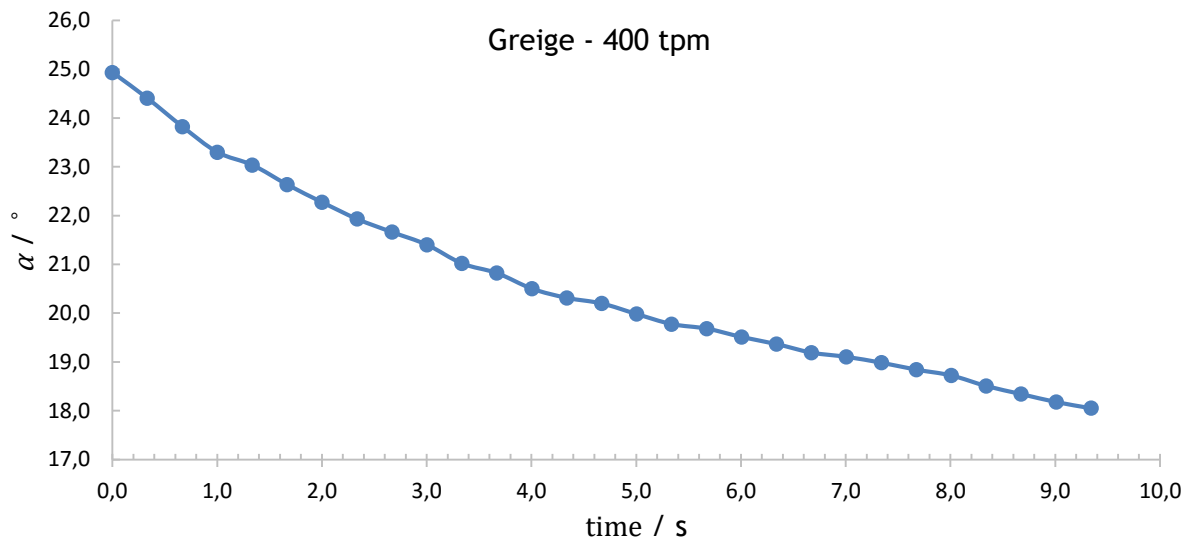


Figure 33 - Helix angle profile for greige 400 tpm cord.

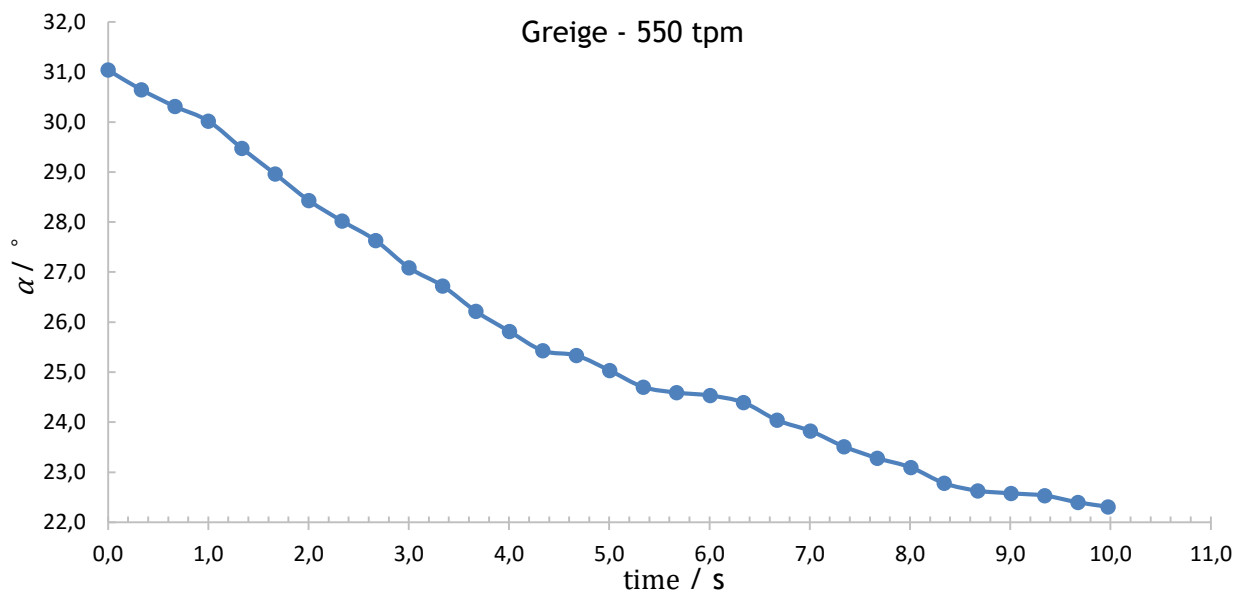


Figure 34 - Helix angle profile for greige 550 tpm cord.

In lower twist level, a more linear and continuous reduction of the helix angle was observed, as in higher twist, the reduction of the helix angle is more dramatic in the beginning of the test. This is owned to the fact that as twist level increases, the structural elongation for small loads is predominant, and afterward the material deformation becomes more principal.

The load-elongation curves of the greige cords presented before are displayed in Figure 35.

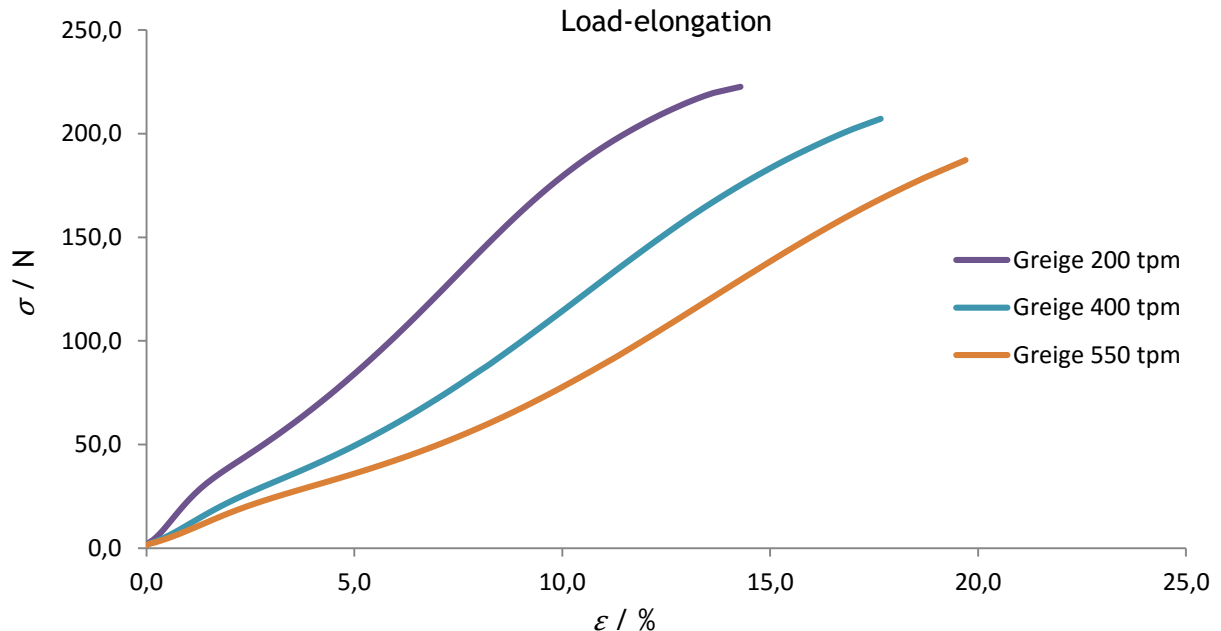


Figure 35 - Load-elongation curves of greige cords with different twist levels.

This process is considerably time consuming, representing a disadvantage to the test method, since each curve takes almost 3 hours of image analysis to be traced. On the other hand, it can be very useful to better understand cord behavior, and it may be convenient in cases where more unconventional cords are tested.

Dipped Cord

The dipping process, once it also comprises a heat and mechanical treatment, affects greatly the cord morphological characteristics. The objective in the following test was to understand these changes and the influence in the helix angle.

Three PET balanced cords, with different twists, were dipped using the LDU machine. The process was made under the standard impregnation conditions of stretch and temperature. The dip and pre-dip used were also the standard ones, used in PET cord industrial manufacture.

The results obtained for helix angle at the pre-tension, breaking moment, LASE 2 % and LASE 4 % are presented in Table 6. Besides the dipped cord values, the greige cord with the same twist level are also presented, in order to allow comparison before and after the dipping process.

Table 6 - Twist level influence in the helix angle in dipped cords.

Cord		Pre-tension		LASE 2 %		LASE 4 %		Breaking		Maximum Load		Maximum Elongation	
Type	Twist / tpm	$\alpha / ^\circ$	$s / ^\circ$	$\alpha / ^\circ$	$s / ^\circ$	$\alpha / ^\circ$	$s / ^\circ$	$\alpha / ^\circ$	$s / ^\circ$	Load / N	s / N	$\varepsilon / \%$	$s / \%$
Dipped	200.00	11.52	0.09	10.87	0.15	10.36	0.09	9.31	0.09	205.43	2.92	13.08	0.30
Dipped	400.00	22.65	0.21	20.78	0.13	19.92	0.12	18.36	0.08	189.66	1.87	15.84	0.21
Dipped	550.00	30.73	0.20	29.71	0.23	28.37	0.18	23.76	0.18	163.48	6.63	18.33	0.80
Greige	200.00	12.67	0.44	11.02	0.32	10.37	0.23	9.04	0.13	222.65	1.24	14.28	0.33
Greige	400.00	25.18	0.40	23.22	0.35	21.20	0.35	18.09	0.38	207.09	2.91	17.66	0.53
Greige	550.00	32.08	0.21	29.32	0.21	27.23	0.22	22.54	0.26	187.30	2.80	19.70	0.59

An increase in the helix angle as the twist level increase was also registered in all the points studied. The dipping process leads to a reduction in the helix angle at pre-tension. This can be justified by the net stretch applied in the dipping process, in this case, 1.5 %. At the breaking point, the helix angle is superior in the dipped cords than in the greige on. In other words, the variation in the helix angle is considerably smaller in the dipped cord rather than in the greige state. This can also be linked with the reduction in maximum elongation after the dipping process, as can also be seen in Figure 36. As expected, the dipping process reduces the cord the maximum load.

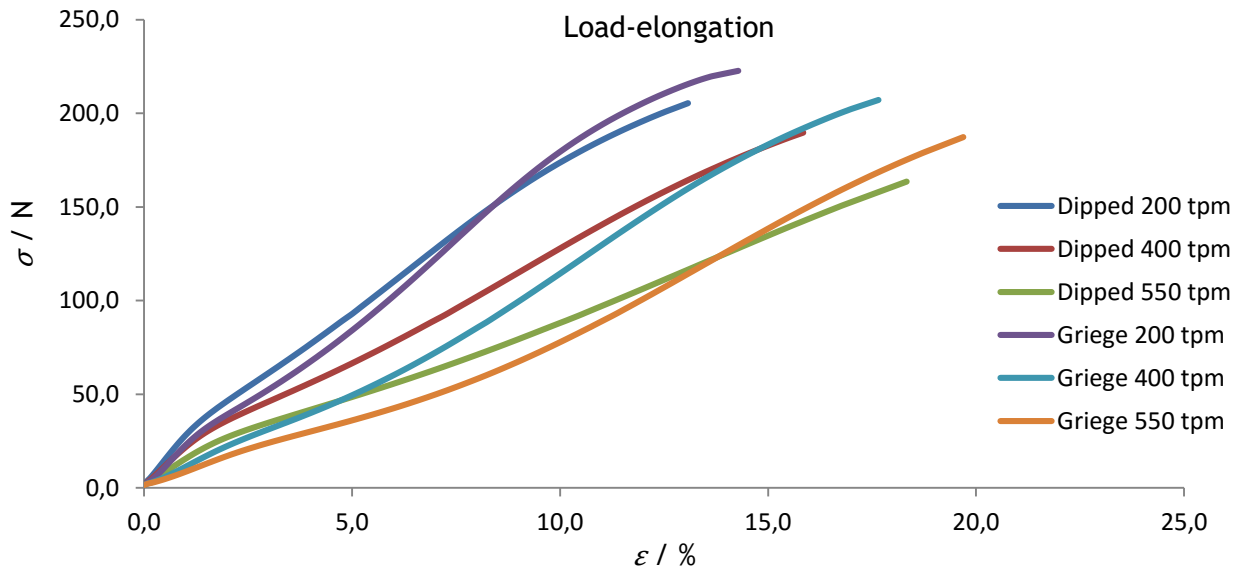


Figure 36 - Load-elongation curve of dipped and greige cords with different twist level.

To better understand and visualize the effect of the dipping process in the helix angle, the helix angle profiles for the greige and dipped cords were determined and are presented in Figure 37, 38 and 39.

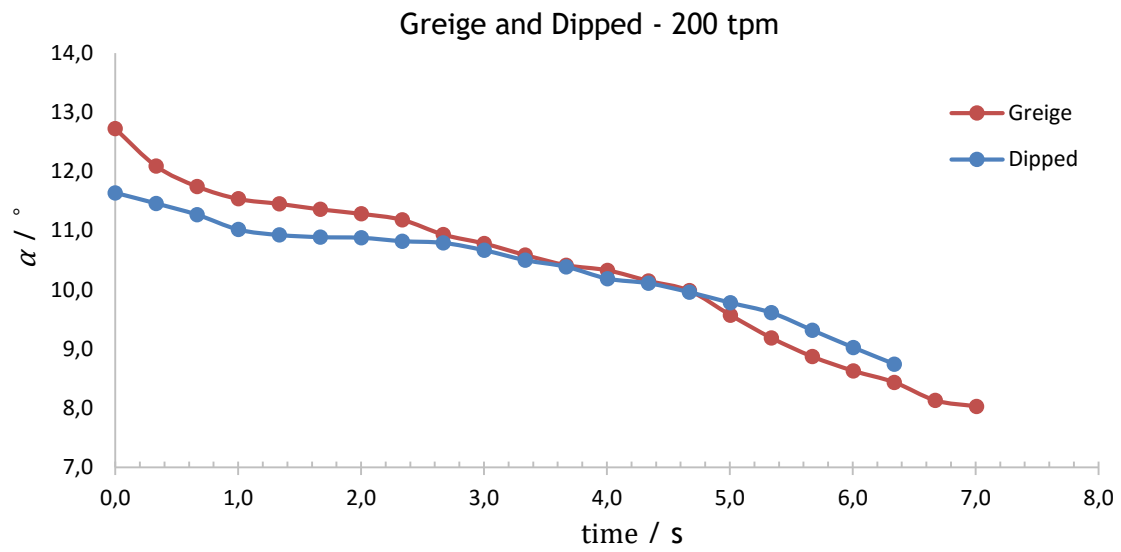


Figure 37 - Helix angle profile for greige and dipped 200 tpm cord.

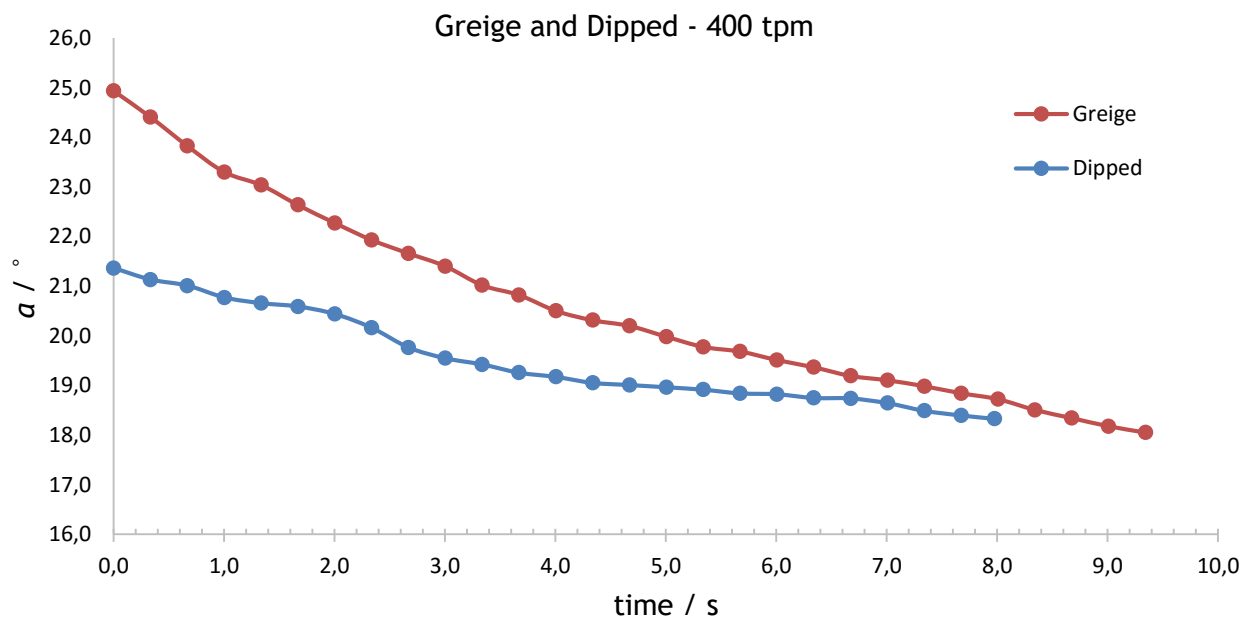


Figure 38 - Helix angle profile for greige and dipped 400 tpm cord.

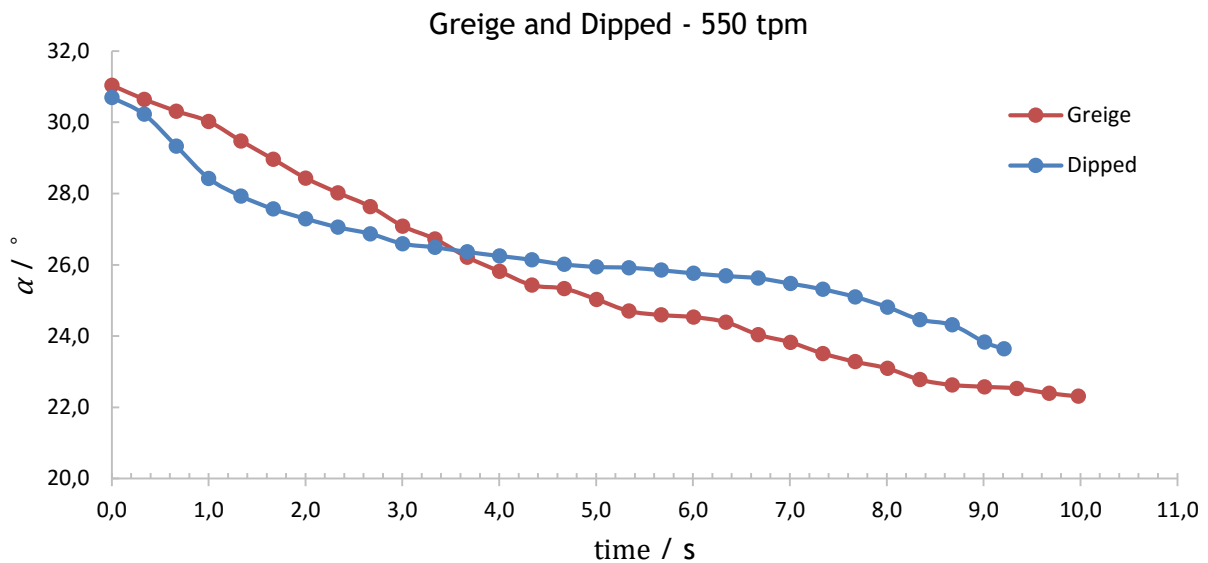


Figure 39 - Helix angle profile for greige and dipped 550 tpm cord.

It is undisputed that the dipping process diminishes the helix angle development. Nevertheless, for higher twist, the predominance of the structural deformation for lower loads is still visible, resulting in a higher rate of helix angle variation.

Other applications

Through all the previously performed test, the camera was kept at the same height, in order to record all tests at the same distance relatively to the inferior Zwick arm. The deformation on the cord is not homogeneous in all its length, and if the camera was not recording at the same height in all tests, the data could not be compared. To study the variation of the helix angle along the entire cord length a ruler was placed sideways to the cord sample. Then similar cords were tested, recording the video at different camera heights. The results from each video sample were then overlapped. Helix angles 0.5 cm apart were then measured in the entire length of the cord throughout the test. To help the visualization, and because the cord length increase as the test develops, the values of the distance were normalized by the total length of the yarn in the respective moment (L). The result is presented in Figure 40. This test would not be of any interest if the camera allow the recording of the entire length during the test.

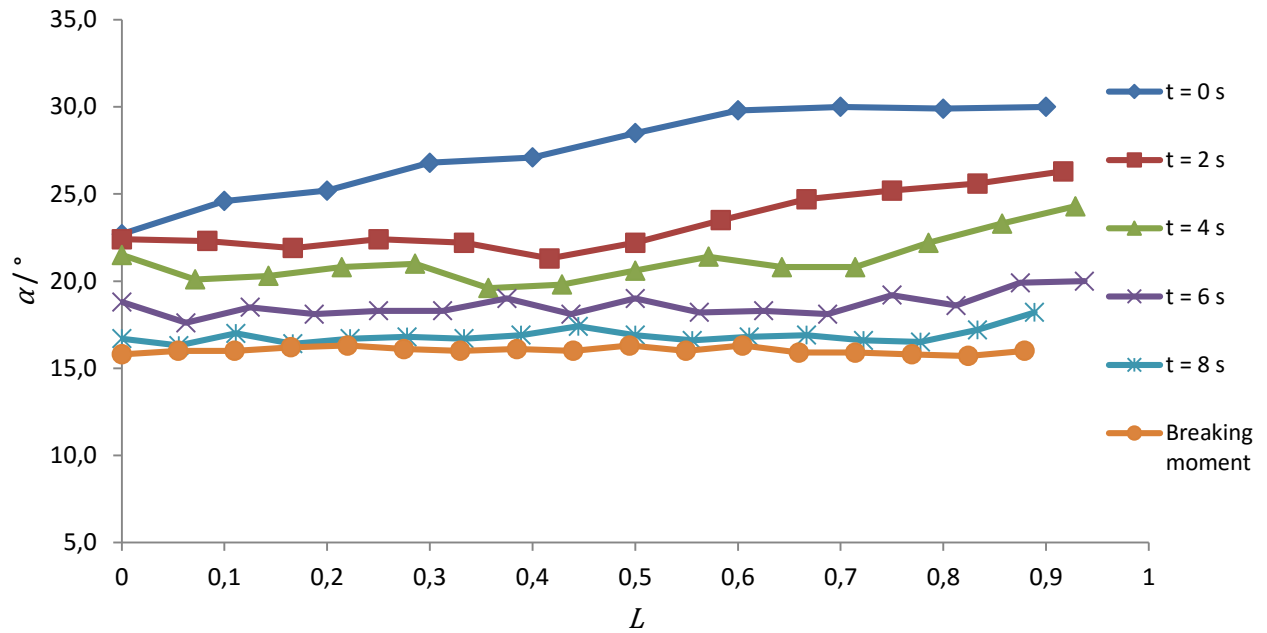


Figure 40 - Normalized helix angle profile at different times.

The only conclusion that can be acquired from this test is that the cord does not deform equally in its entire length. Although it tends to reach the same helix angle in its entire length at the moment of break.

As explained before, a mechanical hysteresis was performed by subjecting a cord Nylon dipped cord to 50 load-unload cycles. The result is presented in Figure 41.

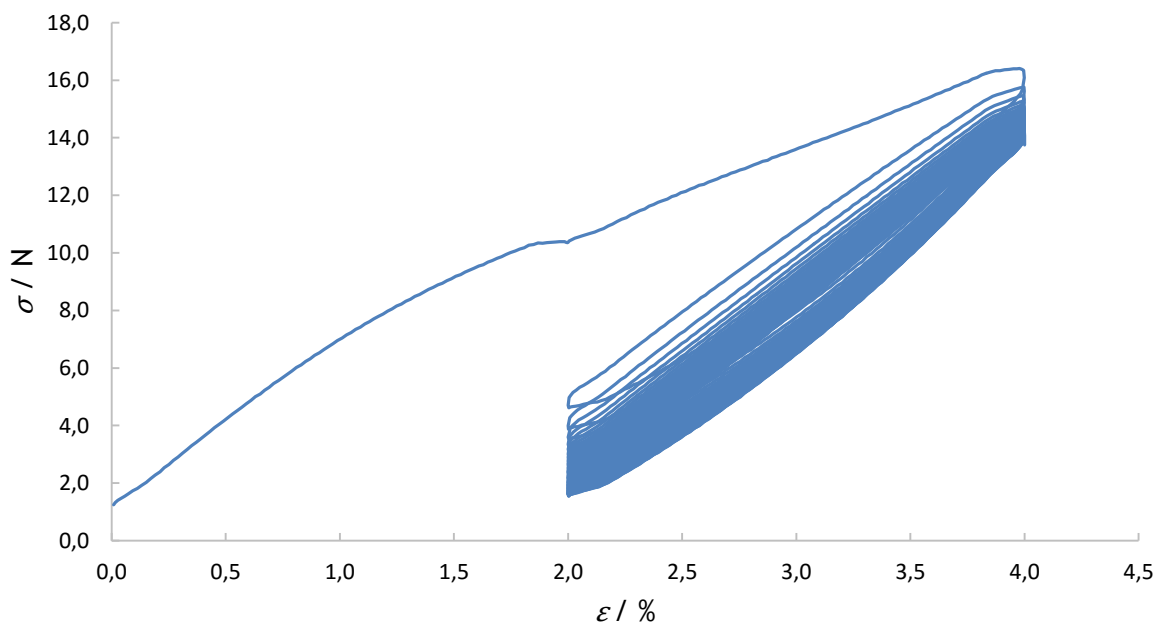


Figure 41 - Nylon mechanical hysteresis.

The helix angles were measured in all cycles at lowest and highest elongation. The goal is to study if there is a conservation of the helix angle along the test. The helix angle evolution at 2 % elongation is presented in Figure 42 and at 4 % elongation in Figure 43.

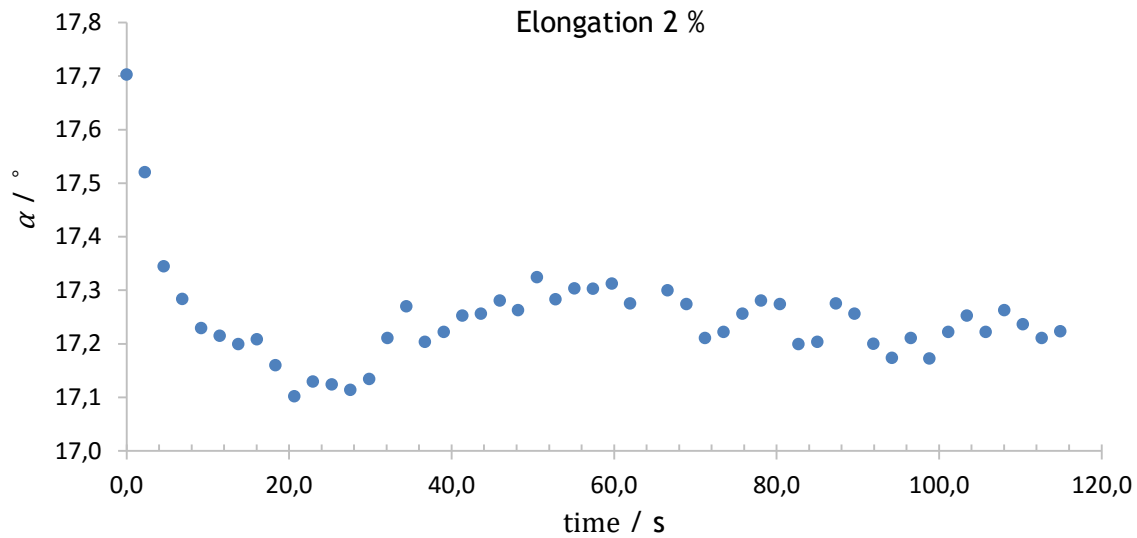


Figure 42 - Helix angle at 2 % elongation.

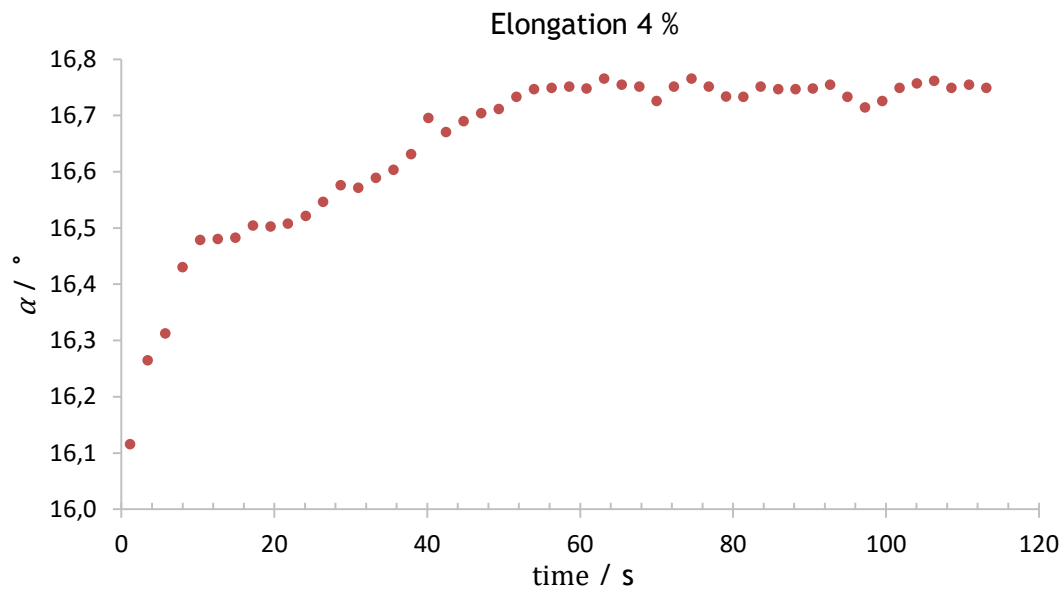


Figure 43 - Helix angle at 4 % elongation.

A cord adaptation to the mechanical solicitation at the beginning of the test is noticeable, as the helix angle slightly changes towards a stable value. Although, to better understand this phenomenon and obtain further conclusions, more tests must be carried.

Finally, one more subject has to be addressed. The breaking mechanism of a cord is an area of interest in the textile cord study. But as the cord is subjected to a high load, when it breaks, the remaining cord parts are projected with a high speed. In order to record this phenomena, a high frame rate is required, possibility up to 1000 fps. Besides that, the cord does not always break at the same spot, remaining always a change of it being out of the recorded area.

Once the fastest camera available for testing is capable of 30 fps, the mechanism of break on a balanced cord was never captured, as displayed in Figure 44. To exemplify what is intended, a hybrid aramid and PET cord was recorded. Since in this case the PET yarns break before the aramid, after the break the aramid keeps the cord together, and therefor of possible recording. The frame-by-frame result is presented in Figure 45.



Figure 44 - Frame-by-frame cord breaking mechanism.

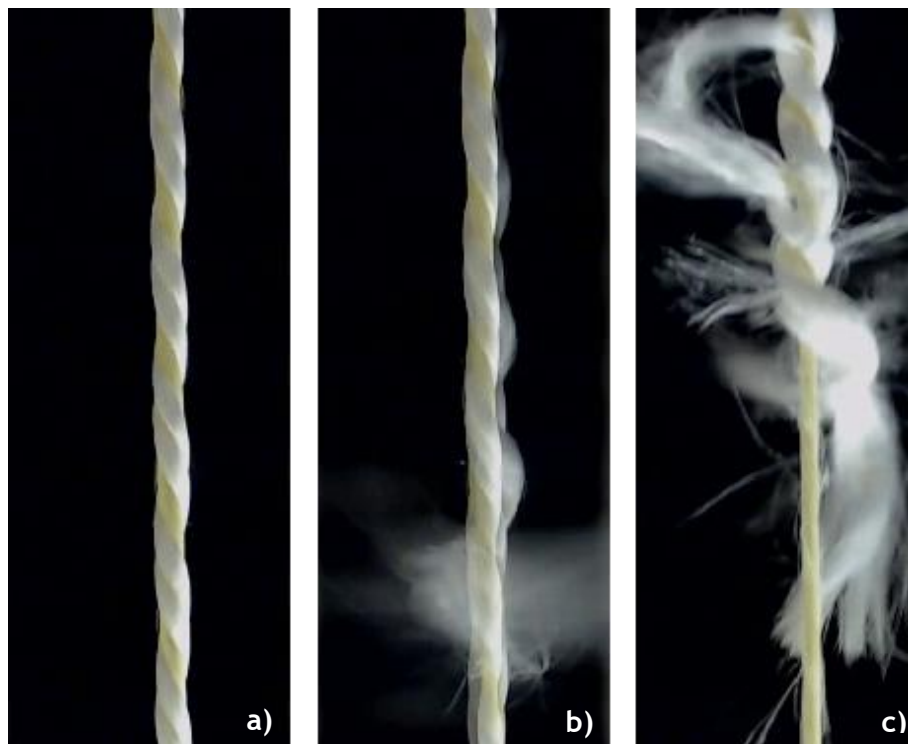


Figure 45 - Frame-by-frame cord breaking mechanism on hybrid cord.

5 Conclusions

A test method for visualizing textile cord elongation and analyzing the helix angle was developed. The goal was to build a tool that enables to study and to comprehend the cord mechanical and morphological behavior when subjected to mechanical solicitations.

The test method installation and recording conditions were studied and optimized, allowing the obtainment images with the sufficient quality to further image analysis. The image analysis is able to provide trustworthy measurements of the cord helix angle development along different mechanical tests. The study of the repeatability and operator influence in the value of the measured helix angle indicate that the analysis method is coherent and consistent, supporting its utilization in the textile reinforcement characterization.

Besides the quantitative information provided by the test method, qualitative information about the materials tested can be also obtained. It allows the operator to better understand the tested cord behavior and properties such as cord regularity and morphological homogeneity.

The main obstacle of this test method is the time required to perform the image analyses, once it can go up to 5 hours for a detailed frame-by-frame measurement. The solution found was to study only specific points of mechanical interest as the standard test.

The standard test consists in the measurement of the helix angle of representative points such as LASE 2 %, LASE 4 %, pre-tension and breaking moment. The helix angle increase as the twist level increase for all the tested cords in the same conditions. Higher twist level leads to higher maximum elongation but lower maximum load.

The influence of the dipping process in the helix angle was studied. Due to the heat and mechanical treatment, the initial helix angles are reduced when the cord is impregnated. On the other hand, the total variation of the helix angle along the tensile tests is reduced.

It was also possible to verify that lengthwise the cord is not deformed equally, but tend afterwards to have the same helix angle when near the break. The regular breaking mechanism could not be recorded with the material available.

This test method will not revolutionize the way textile reinforcements are produced, nether will it be performed in every load-elongation test. But it is a useful tool that allows further knowledge and understanding of the properties and behavior of the cords tested, and may aid in the study of less conventional cords such as unbalanced, asymmetrical and hybrid cords.

6 Project Assessment

The main objective of this project was to develop a working test method that enable visualization and image analysis of textile cords. This objective was fulfilled, once it is possible to measure the helix angles of textile cords during mechanical tests. The results obtained match the expected outcome, allowing to consider the test method coherent and feasible.

6.1 Limitations and future work

There are some aspects in which this method can be improved. The first is the application of the camera elevation device that will allow the camera to follow the same helix throughout the test, allowing a more representative value of the helix development.

The time required for image analysis is the most limiting problem with the developed test method. Therefore, the creation of an automatized analysis system to measure the helix angle may be a focus of future work. In that case, fully controlled illumination is normally needed, and would require the construction of a black case in the Zwick machine, that probably will also increase the difficulty of test operation.

Finally, the use of thermographic cameras could also bring advantages in the breaking point study. Material deformation is usually an exothermic process, and will possibly lead to an increase in temperature where the rupture occurs. The use of a thermographic camera with an adequate sensibility may detect this phenomena and enable its study.

6.2 Final assessment

This project intertwine the consummation of the academic education and the first working experience in the industry. It was a demanding task but undoubtedly rewarding, as the problems were solved and solutions arose. The final result is a working method that can be used in the development of better and safer technology for tires.

7 References

1. Rodgers, B. and W. Waddell, *Tire Engineering*, in *The Science and Technology of Rubber*. 2013, Elsevier Science.
2. Continental-AG, *Tyre Basics - Passenger Car Tyres*. 2009.
3. Fung, W., M. Hardcastle, and T. Institute, *Textiles in Automotive Engineering*. 2001: Technomic.
4. Lindenmuth, B.E., *An overview of tire technology*, in *The Pneumatic Tire*. 2005: National Highway Traffic Safety Administration.
5. Moodley, S.a.A., D., *An analytical study of vehicle defects and their contribution to road accidents*. 2008, Department of Civil Engineering & Surveying, Durban University of Technology.
6. Kumar, R.S., *Textiles in Automobiles*, in *Textiles for Industrial Applications*. 2013, CRC Press.
7. Ford, T.L., F.S. Charles, and S.o.A. Engineers, *Heavy Duty Truck Tire Engineering*. 1988: Society of Automotive Engineers.
8. Heisler, H., *Tyres*, in *Advanced Vehicle Technology*.
9. Evans, M.S., *Tyre Compounding for Improved Performance*, ed. R.T. Ltd.
10. Continental Corporation. [cited 2015 September 29]; Available from: www.contimaboronline/gca.
11. Inc., C.C., *North America, Europe and the World Top Suppliers*, in *Automotive News*. 2015.
12. Continental-AG, *Mobility Is The Future - Annual Report*. 2014.
13. Aytaç, A., B. Yilmaz, and V. Deniz, *Effect of twist level on tyre cord performance*. *Fibers and Polymers*, 2009. 10(2): p. 221-225.
14. Miravete, A., *3-D Textile Reinforcements in Composite Materials*. 1999: Elsevier Science.
15. Roylance, D., *Stress-Strain Curves*. 2001, Massachusetts Institute of Technology.
16. ASMI, *Introduction to Tensile Testing*, in *Tensile Testing*. 2004.
17. Fanguerio, R.S., F., *Yarn imaging and advances in measuring yarn characteristics*, in *Technical Textile Yarns*. 2010, Woodhead Publishing Limited.
18. Burrowes, G. and B. Rodgers, *Reinforcing Materials in Rubber Products*. The Goodyear Tire and Rubber Company, 2010.
19. Wahl, G., *Basic of reinforcement Materials for Tires*, ed. Continental. 1999.
20. Wootton, D.B., *The Application of Textiles in Rubber*. 2001: Rapra Technology.
21. McDonel, E.T., *Tire Cord and Cord-to-Rubber Bonding*, in *The Pneumatic Tire*. 2005: National Highway Traffic Safety Administration.
22. Gent, A.N., *Mechanical Properties of Rubber*, in *The Pneumatic Tire*.
23. Mukhopadhyay, S.K.P., J.F., *Automotive Textiles*. 1999.
24. Kandagor, V.B., G., *Synthetic polymer fibers and their processing requirements*, in *Advances in filament yarn spinning of textiles and polymers*, D. Zhang, Editor. 2014, Woodhead Publishing Ltd: The textile institute.

25. Baird, D.G., *Polymer Processing*. Physical Science and Technology. Virginia Polytechnic Institute and State University.
26. Hockenberger, A.S.K., S., *Effect of twist on the performance of tire cord yarns*. Fibre & Textile Research, 2003.
27. Relf, C.G., *Image Acquisition and Processing with LabVIEW*. Image Processing Series, ed. P.A. Laplante.
28. RICOH Company, L. *The mechanism of a digital camera*. Digital Camera Basic Knowledge [cited 2015 December 7]; Available from: http://www.ricoh.com/r_dc/photostyle/knowledge/preparation/digitalcamera.html.
29. Young, I.T.G., J.J.; Vliet, L.J, *Fundamentals of Image Processing*, in *Delft University of Technology*. 2007.
30. Gomes, D., *Influence of the test speed on the Force vs. Elongation Curves of reinforcement materials*, in *Departamento de Química*. 2015, Universidade do Porto.
31. *ASTM D885 / D885M - 10a : "Standard Test Methods for Tire Cords, Tire Cord Fabrics, and Industrial Filament Yarns Made from Manufactured Organic-Base Fibers"*. 2012: Annual Book of ASTM Standards.
32. Roell, Z., *testXpert II*.
33. Barraclough, J., *PhysMo*. 2006.
34. Health, N.I.o., *ImageJ*. 2004.
35. Unit, Q.I.A., *Icy*. 2011.
36. Brown, D., *Tracker - Video Analysis and Modeling Tool*. 2015.
37. SolidWorks, *SolidWorks*. 1993.
38. Feinberg, M., *Basics of interlaboratory studies*. Trends in analytical chemistry, 1995. 14.

8 Attachment I - Test Method Procedure



CONTINENTAL - INDÚSTRIA TÊXTIL DO AVE, S.A.

Zwick: Load-Elongation Test with Video Recording

Installation Setup

USB Cameras (EdmundOptics and LogiTech)

1. Turn Zwick machine ON/OFF switch to ON position.
2. Connect the USB Video Camera to the Zwick Computer.
3. Start *testXpert II* software.
4. Click Zwick frontal control button. The button light will turn on.
5. Attach the clamps to the Zwick machine arms and connect the pressurized air supply tube to the clamps.
6. Go to Load > Test Methods and select the Test Program "1kN_Tensile_Cold_NormalConditions_VideoAnalysis.zp2".
7. Click "Start Position" in the Menu bar (see Figure 46).
8. Click "Force 0" in the Menu bar.
9. Place the cord sample in the clamps.
10. Place the background board behind the cord sample.
11. Place the camera on the tripod, and level the camera.
12. Place the led illumination source in the second tripod. Adjust the light to enhance the helixes.
13. Point the laser to the background, making sure that is within the recorded area.
14. On the secondary menu bar select Video Capture. Right click above the displayed image and select Configure Video Recording. Select Camera Control and focus the camera. Optimize the available parameters if necessary. A clear image with distinguishable helixes should be obtained. Define the recorded videos destination file. Signal the laser beam in the Video Synchronization layout (as exemplified in Figure 47).
15. In the Wizard Menu, set the correct Pre-load (multiply the dtex by 0.05).
16. Start the test.

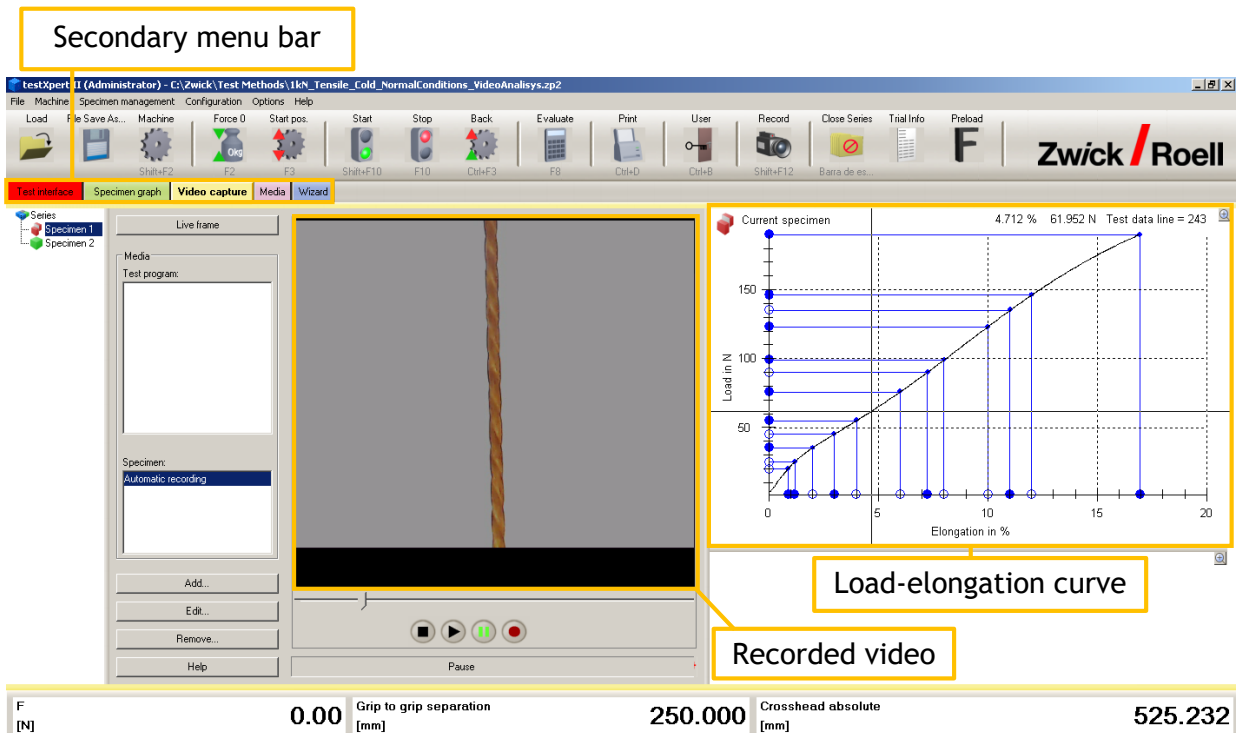


Figure 46 - testXpert user interface for video analysis.

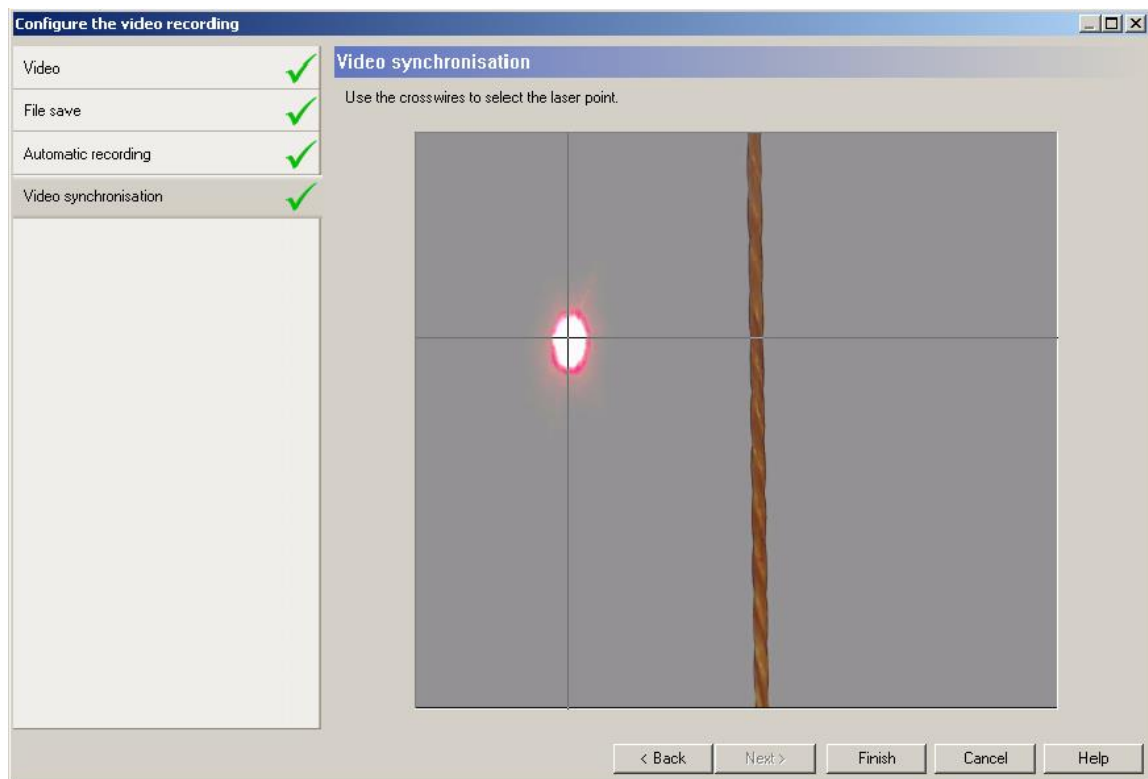


Figure 47 - Video synchronization by laser light detection.

In the case of using a non USB camera, ignore the steps 2, 13 and 14. The camera should be manually focused. Before starting the test, press the recording button in the camera. As soon as the cord breaks, stop the recording.

Image Analysis

1. Start Tracker software, represented in Figure 48.
2. Open the recorded video by File>Open File and select the video.
3. Navigate through the video in the Video Control Bar and determine the frame in which the cord breaks. Right click over the bar and Define as ending frame.
4. Navigate backwards until the beginning and determine the frame in which the cord start the elongation. Right click over the bar and Define as starting frame.

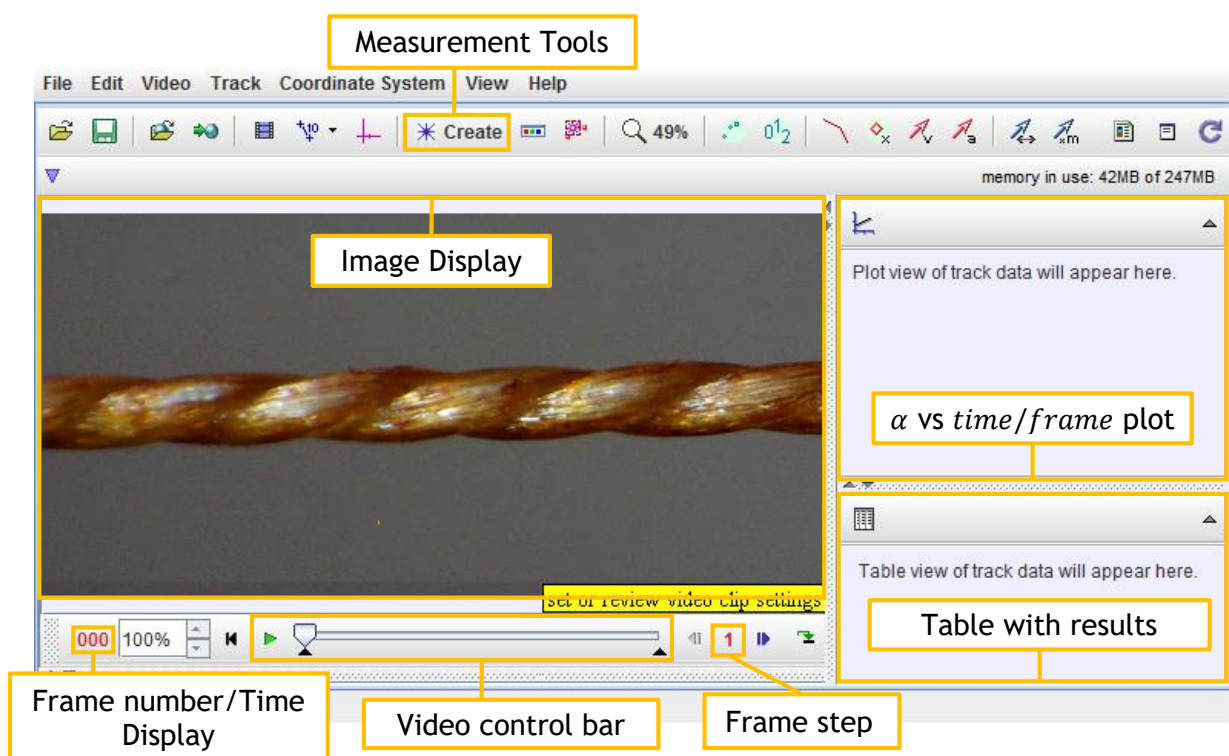


Figure 48 - Tracker user interface.

5. Create a Protractor tool by clicking Create>Measuring Tools>Protractor.
6. Disable the Fix option in the Protractor menu. Change colors and bar thickness if necessary.
7. Align a Protractor arm by the cord axis, as represented in Figure 49 in red points.
8. Set the Protractor vertex above a point where on yarn overlays the other, as represented in Figure 49 as 50.
9. Align the remaining Protractor arm by the yarn axis.
10. Repeat the process to three consecutive helixes.
11. Select the following frame and repeat steps 7, 8, 9 and 10.



Figure 49 - Protractor displacement exemplification.

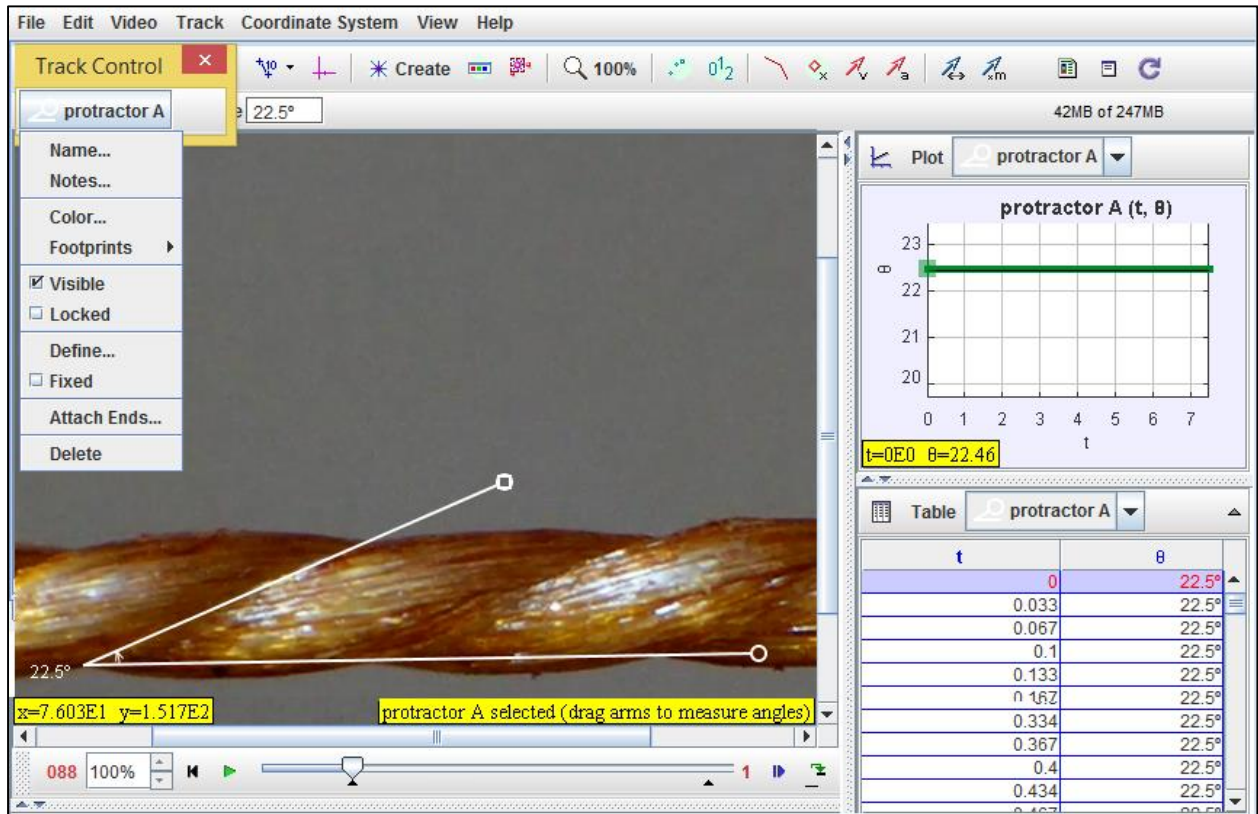


Figure 50 - Helix angle measurement exemplification.

12. When the image analysis is concluded, export the data by clicking File>Export>Data File.